scientific reports

Check for updates

OPEN

Integrated fermentation, downstream processing, and formulation shape the performance of *Bacillus thuringiensis*-based biocontrol agents

Rayan Nasreddine[1], Gül Ayyildiz[1], Zhanerke Amangeldi[2], Cecilia Peralta[5], Asime Filiz Caliskan Keçe[2], Mireille Kallassy Awad[3], Luc Fillaudeau[4], Baltasar Escriche[5] & Dietrich Stephan[1]✉

The performance of *Bacillus thuringiensis* (Bt)-based biopesticides depends not only on their insecticidal proteins but also on the manufacturing process, from fermentation through downstream formulation. However, these stages are often investigated independently, limiting understanding of how process design influences the properties and performance of the final product. This study develops and evaluates a spray-dried formulation of *Bacillus thuringiensis* subsp. *kurstaki* (Btk) strain Lip by characterizing the fermentation growth–sporulation trajectory using controlled physicochemical parameters and off-gas monitoring, relating these dynamics to spore and protein production, characterizing the resulting spray-dried formulation, and evaluating its laboratory bioefficacy, and stability .Btk Lip was produced by submerged fermentation on a wheat bran medium under controlled operating conditions and converted to a spray-dried formulation (Lip-F) designed to enhance application performance and resistance to sunlight degradation, and as a unformulated dried material (Lip-U) that will serve as a control and a baseline for following experiments. Across four fermentations (72 h/batch), off-gas and pO_2 profiles were reproducible and coincided with rapid sporulation (9.0–10.0 log_{10} CFU/mL) and protein accumulation (1.4–1.5 mg/mL). Quality control showed preserved Cry profiles (130 and 60–65 kDa) and comparable Cry densitometry to Delfin® (5.0 ± 1.0 vs. 4.1 ± 0.5 mg/g), with higher total protein in Lip-F (104 ± 15 vs. 61 ± 13 mg/g). Bioassays across pests showed efficacy comparable to Delfin®, with higher potency against *Ostrinia nubilalis* (LC_{50} ratio 2.3; $p = 0.03$). Sunlight exposure improved stability, Lip-F retained 30 ± 6% CFU vs. 1.85 ± 1.18% (Lip-U), preserved Cry integrity, and maintained *Spodoptera frugiperda* mortality (Odds Ratio 0.217 vs. 0.0386).

Keywords *Bacillus thuringiensis* subp. *kurstaki* Lip, Median lethal concentration, Morphological characterisation, Formulation stability, Sunlight stress

The increasing global demand for environmentally safer, and more sustainable pest control strategies has intensified interest in biopesticides as alternatives to conventional chemical insecticides[1]. Growing concerns related to environmental contamination, resistance development, and regulatory constraints have accelerated the integration of biological control agents into modern integrated pest management (IPM) programs. Within this context, microbial plant protection products have gained relevance due to their target specificity, compatibility with IPM principles, and favourable safety profiles.

[1]Julius Kühn Institute (JKI)–Federal Research Centre for Cultivated Plants, Institute for Biological Control, Dossenheim, Germany. [2]Department of Plant Protection, Faculty of Agriculture, Çukurova University, Adana, Türkiye. [3]Functional Genomic and Proteomic Laboratory, UR- EGP, Faculty of Sciences, Université Saint- Joseph de Beyrouth, Beirut 1104 2020, Lebanon. [4]Toulouse Biotechnology Institute, Bio & Chemical Engineering, TBI, Université de Toulouse, CNRS, INRAE, INSA, Toulouse 31077, France. [5]Laboratory of Biotechnological Pest Control (CBP), Department of Genetics, Institute of Biotechnology and Biomedicine, University of Valencia, Valencia 46100, Spain. ✉email: dietrich.stephan@julius-kuehn.de

Among those biocontrol agents, *Bacillus thuringiensis* (Bt) represents the most widely used, and commercially successful example, with more than half a century of large-scale agricultural application. Bt is a Gram-positive, spore-forming bacterium that produces parasporal crystalline inclusions during sporulation. These inclusions are composed primarily of insecticidal crystal (Cry) proteins, which constitute the main bioactive component of Bt-based products[2]. Upon ingestion by susceptible insects, Cry proteins are solubilized, and proteolytically activated in the alkaline environment of the larval midgut. Activated toxins bind to specific epithelial receptors, form pores in the gut membrane, and ultimately induce osmotic lysis, and insect death[2]. This highly specific mode of action underlies the strong selectivity, and favourable toxicological profile of Bt formulations.

Amid the various Bt subspecies, *Bacillus thuringiensis* subsp. *kurstaki* (Btk) is the most applied due to its efficacy against a wide range of lepidopteran pests. Btk-based products used to control economically important species such as *Spodoptera frugiperda* (J.E. Smith), *Spodoptera exigua* (Hbn.) (Lepidoptera: Noctuidae), *Grapholita molesta* Busck (Lepidoptera: Tortricidae), *Ostrinia nubilalis* Hbn (Lepidoptera: Pyralidae), and *Phthorimaea absoluta* Meyrick (Lepidoptera: Gelechiidae)[3–5]. These pests affect major crops including maize, vegetables, and fruit trees, and represent persistent challenges to agricultural productivity across diverse agroecosystems.

While the biological activity of Bt, and its Cry proteins has been extensively characterised, the practical performance of Bt-based products depends not only on intrinsic toxicity but also on formulation, and processing parameters. In industrial production, Bt is cultivated in submerged systems, after which the spore-crystal suspension must be recovered, stabilized, and formulated into a usable product. The physicochemical conditions during culture, including temperature, pH, dissolved oxygen availability, and nutrient composition, strongly influence each phases: oxidative growth, nutritional limitation then sporulation efficiency, and Cry protein synthesis[6]. Variability at this stage can directly affect the quality and consistency of the material entering downstream processing steps. Despite this sequential dependence, upstream bioprocess optimization and downstream formulation development are commonly investigated independently. Consequently, the extent to which fermentation-derived material properties influence the performance of the final formulated product remains insufficiently understood.

Drying constitutes a critical stage in the production of Bt formulations, as it converts fermentation broths into solid products suitable for storage, transport, and resuspension for field application. Spray drying is one of the most commonly used industrial techniques for this purpose, owing to its scalability, operational flexibility, and ability to produce free-flowing powders with controlled moisture content[7]. In spray drying, liquid feed is atomized into fine droplets that are rapidly dried in a stream of heated air, resulting in short residence times, and high throughput. Compared with alternative drying methods, spray drying allows continuous operation and facilitates the incorporation of formulation excipients, making it particularly attractive for large-scale biopesticide production[8].

Beyond its role in dehydration, spray drying apply a profound influence on the physical properties of the resulting powder, especially particle size distribution, morphology, and surface characteristics. These attributes are increasingly recognized as key determinants of formulation performance, yet they are often treated as secondary considerations in efficacy-driven studies. Particle size, and shape affect powder flowability, dispersibility, wettability, and suspension behaviour, all of which influence how Bt formulations are prepared, and applied in practice[9]. In aqueous suspensions, particle size distribution governs sedimentation kinetics, and the spatial distribution of particles within spray tanks, thereby affecting dose homogeneity, and delivery of the active ingredient[10].

Particle morphology also plays a critical role in determining how Bt formulations interact with water during reconstitution. Irregularly shaped or aggregated particles may settle rapidly or form compact sediments, whereas finer, and more homogeneous particles tend to remain suspended for longer periods[11]. These differences can translate into variable exposure of target insects to spores, and Cry proteins, even when nominal application rates are identical. Thus, formulation-induced changes at the particle scale can modulate the effective bioavailability of Bt toxins independently of their intrinsic potency.

Despite the recognized importance of particle-scale properties in formulation science, many studies assessing Bt efficacy rely predominantly on biological endpoints such as LC_{50} values derived from laboratory bioassays. While such metrics are essential for comparing intrinsic toxicity, they provide limited insight into the mechanisms by which formulation structure influences insecticidal performance[12]. As a result, differences in efficacy between products are frequently attributed solely to variations in Cry protein content or strain composition, without considering the contribution of particle morphology, size distribution, or suspension stability.

Recent work has begun to highlight the importance of formulation structure in determining Bt performance[13] demonstrated that reducing particle size, and optimizing formulation characteristics could enhance Bt bioefficacy by improving dispersion, and availability of the active ingredient[14]. However, systematic studies that integrate upstream bioprocess parameters, particle-scale characterisation, suspension behaviour, and multi-species bioassays remain limited. Few investigations have explicitly linked morpho-granulometric properties of Bt formulations to sedimentation dynamics, and comparative bioefficacy across different lepidopteran pests. A more integrated perspective is therefore needed to understand how successive production and formulation steps collectively influence the quality and performance of Bt-based biocontrol products.

Addressing these gaps requires a process–structure–function framework in which bioperformances, formulation-induced particle properties, and biological efficacy are considered as interconnected elements rather than isolated variables. Accordingly, the aim of this study was to develop, and comprehensively evaluate a spray-dried Btk formulation Lip-F, by integrating upstream culture characteristics with downstream formulation properties, and biological performances. Specifically, this work aimed: (i) to characterize key physicochemical parameters of the submerged cultures, and their influence on spore, and protein production to scale-up bioprocess, (ii) to assess particle morphology, size distributions, and sedimentation behaviour of the resulting formulations using complementary analytical techniques, and (iii) to evaluate the laboratory bioefficacy of Lip-F

across multiple lepidopteran pests in comparison with a commercial reference product, Delfin® WG (Certis, Columbia, MD, USA) as well as its stress-tolerance under sunlight simulation. By integrating fermentation performance, particle-scale characterization, suspension behaviour, and insecticidal activity, this study provides an integrated evaluation how successive production and formulation steps shape the physicochemical and biological performance of Bt-based biocontrol products.

Experimental methods

B. thuringiensis subsp. *kurstaki* Lip mass production

Bacillus thuringiensis subsp. *kurstaki* strain Lip, isolated by El Khoury et al.[15], and described by Fayad et al.[16] was used. The strain was preserved in the Microbank™ storage system (Pro-Lab Diagnostics, Canada) at -80 °C.

For inoculum preparation, one colony was inoculated into 25 mL Lysogeny Broth (LB) media containing 1% (w/v) tryptone (Carl Roth GmbH, Karlsruhe, Germany), 0.5% (w/v) yeast extract (Carl Roth GmbH, Karlsruhe, Germany), 1% (w/v) sodium chloride (Carl Roth GmbH, Karlsruhe, Germany), in a 250 mL Erlenmeyer flask, and incubated at 30 °C, 200 rpm for 12–14 h to the mid-exponential phase ($OD_{600} \approx 1.0$)[14]. Cultures ($n = 4$) were performed in batch mode (V = 3 L) in a 5 L BioBench single bioreactor (BioStream International B.V., Netherland) fully instrumented, and regulated (temperature, pH, foam level, dissolved oxygen, mixing rate, air flow), and online variables were automatically operated through the Biostream Operating System (BOS). The culture media was a 73.4 gram of humid matter per litre (ghm/L) suspension of wheat bran (WB) (mix 60:40 w/w ratio with class 2 (500–850 µm), and class 3 (250–500 µm) (ROPOMIX Rol, and Pöppelmann oHG, No. 08/23/33, 48161 Münster, Germany) described previously by Nasreddine et al.[14].

Oxidative axenic submerged cultures were carried out at 30 ± 0.5 °C with constant aeration (Qair = 1.6 nL/min equivalent to VVM = 0.53 L/(L/min)), regulated pH 7.0 ± 0.1 (regulation with 1 M NaOH (Carl Roth GmbH, Karlsruhe, Germany), and 1 M HCl (Carl Roth GmbH, Karlsruhe, Germany), and a nominal agitation speed at 600 rpm. Dissolved oxygen (DO) level was regulated above 25% air saturation (mixing rate max 850 rpm), and an antifoam (Antifoam 204, Sigma-Aldrich, St. Louis, USA) was automatically dosed as needed[14]. Online pH, and DO sensors (Hamilton EasyFerm Plus pH, and Hamilton VisiFerm DO Arc, Hamilton Bonaduz AG, Bonaduz, Switzerland) realized stable, and consistent readings throughout 72 h. Off-gas O_2, and CO_2 concentrations were monitored online using the BOS, whose base unit can be configured with integrated off-gas analysers – in this setup – a BlueSens BlueInOne Ferm module was used for simultaneous O_2, and CO_2 measurement.

Aseptic offline samples (~6 mL) were collected along cultures at defined times (each 4 h until 24 h, and each 12 h until 72 h). Every sample was separated into aliquots for bio-performance analysis. Cell and spore concentrations were determined by colony-forming-unit (CFU) counts[17]. Protein content was determined by the Bradford assay (Bio-Rad Laboratories, Hercules, USA)[18]. This comprehensive data structure served as the basis for developing the hybrid model that bridged mechanistic growth kinetics with data-driven adjustments towards the estimation of real-time biomass.

Downstream process (DSP), and formulation preparation

After cultivation, the broth containing Lip spores, endotoxin crystals, cell debris from lysis, and unconsumed substrates was processed. After a primary decantation, the clarified broth was pumped out using harvested, and filtered under sterile conditions (dead-end filtration, sieves / cut-off = 75 µm) then permeate was transferred into sterile bottles, and centrifuged at 8000 g for 20 min at 4 °C (Eppendorf 5810 R, Hamburg, Germany)[14]. The supernatant was tipped off, and the wet concentrated pellet kept for the formulation steps. A representative sample (2 g wet pellet) was used to quantify the dry matter content (Sartorius MA-150 moisture analyser, Sartorius AG, Göttingen, Germany). The sample was dried at 105 °C until constant weight, and the dry weight fraction was used to estimate the active ingredient concentrations (spores, crystals), and normalised its content into final formulation.

For formulation preparation (Lip-F), 70.60 ± 1.45 g of concentrated pellet, corresponding to 14.91 ± 0.91 g of dry matter (gdm) equivalent (21.12 ± 1.13% dry matter) was dispersed under 150 rpm, 25 °C until homogeneity in a 50 mL suspension of Titanium dioxide (TiO_2, 5mM, coarse powder size: 700–800 µm, Carl Roth GmbH, Karlsruhe, Germany). Lactose powder ($D_{[4,0.3]}$ = 50 µm, and spread: <10 µm: 10%, 10–100 µm: 40%, and 100–400 µm: 50%, Dm-Drogerie Markt GmbH + Co. KG, Karlsruhe, Germany) was added, and volume adjusted to 300 mL with autoclaved deionized water to obtain a processable viscosity for spray drying. On a dry-matter basis, the formulated product (Lip-F) contained 85% w/w active ingredient, 15% w/w of lactose, and TiO_2. In parallel, an unformulated reference material (Lip-U) was prepared by spray drying the same Lip biomass without any co-ingredients, using the same processing workflow, to provide a baseline for subsequent physical characterisation, and sunlight stability assays.

The aqueous suspension was spray-dried (Büchi Mini Spray Dryer S-300, Büchi Labortechnik AG, Flawil, Switzerland) with a two-fluid nozzle (Nozzle cap = 2.2 µm, Nozzle = 1.8 µm), and cyclone separator. The operating conditions were stabilized with distillated water at 180 °C, and 90 °C for air inlet, and outlet temperatures respectively, with liquid feed rate at 2 mL/min[19], spray gas at 800 L/h, drying gas 35 m^3/h, and atomization at atmospheric pressure (filter pressure = 0.11–0.13 bar) indicating consistent airflow and no filter clogging during the drying process. Under steady-state conditions, the suspension was fed, and the feeding rate slightly increased at 2.5 mL/min to maintain product temperature constant. The operation was observed until the feed solution is entirely atomized, and the formulated powder collected in the product collector vessel under the cyclone. The sterile dried material was transferred into 50 mL Falcon™ polypropylene tubes. The overall yield is measured, and the samples kept in covered containers in dark dry places until subjected to analysis as described in Fig. 1.

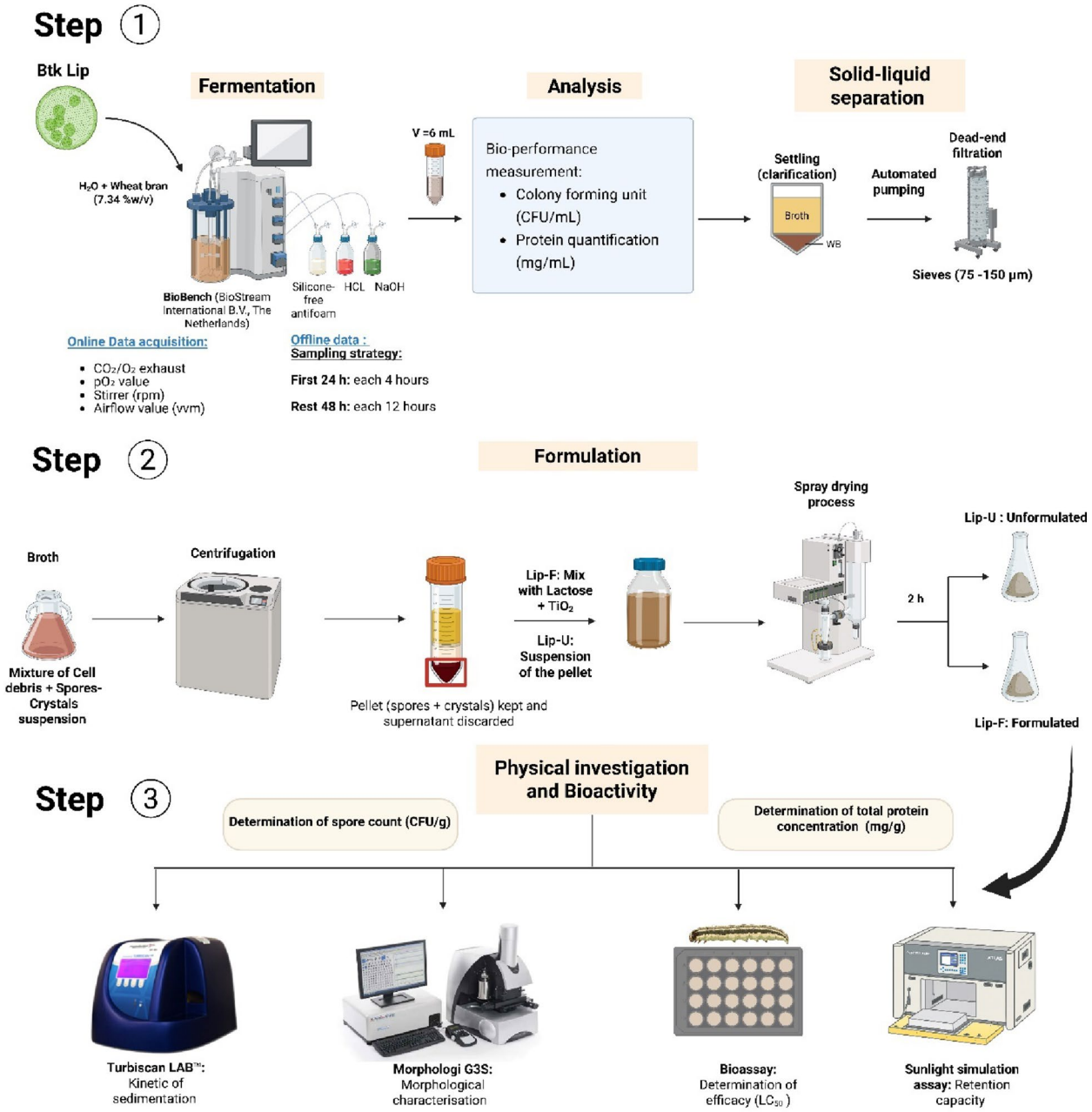


Fig. 1. Overview of the workflow used to produce and evaluate formulation from *Bacillus thuringiensis* subsp. *kurstaki* strain Lip. Step 1: Submerged Btk culture with wheat bran-based medium in bioreactor, and clarification (settling), and dead-end filtration. Step 2: Permeate centrifugation, centrifugation pellet resuspension with co-formulant. Step 3: Formulated, and un-formulated powder obtained by spray drying, and followed by quality control, and performance assessment. Created in BioRender. Nasreddine, R. (2026) https://BioRender.com/wlbmils.

Bioperformances, physical investigations, and bioefficacy

Colony-forming unit count

For the fermentation broth, and formulated products, spores were counted after plating onto Lysogeny Broth Agar (LBA) media (1% (w/v) tryptone (Carl Roth GmbH, Karlsruhe, Germany), 0.5% (w/v) yeast extract (Carl Roth GmbH, Karlsruhe, Germany), 1% (w/v) sodium chloride and 1.5% (w/v) agar-agar (Carl Roth GmbH, Karlsruhe, Germany) in Petri dishes. The number of colony-forming units (CFU) associated with spores was determined by heating the samples at 80 °C for 10 min, to eliminate vegetative cells, following the method of Sanders[17], and Warda et al.[20] using a Thermocell Cooling & Heating Block (model CHB-202; Bioer Technology, Hangzhou, China). Serial ten-fold dilutions (10^{-1}-10^{-6}) were then prepared, and plates were inoculated using a spiral plater (Whitley WASP 2 spiral plater; Don Whitley Scientific Ltd., Bingley, UK). Subsequently, the Petri dishes were incubated for 16 h at 30 °C then colonies were counted.

Bradford quantification

The Bradford assay was used to quantify the total soluble protein content of each preparation, providing a quantitative measure for comparison among formulations prior to qualitative characterization by SDS-PAGE. The total protein content was quantified using the Bradford colorimetric method, based on the dye–protein binding to a dye reactant[18]. Samples were washed with 1 M NaCl, and cold sterile deionized water, then the total protein content was solubilised using 50 mM NaOH at 30 °C with shaking for 2.5–3 h[15]. After centrifugation, aliquots of supernatant were transferred to 96-well microplates, mixed with the Quick Start™ Bradford Protein Assay reagent (Bio-Rad Laboratories Inc., Hercules, CA, USA), and incubated in the dark for 10 min. Absorbance was measured at 595 nm using a FLUOstar® Omega microplate reader, and protein concentrations were calculated using, and the linear regression of the standard curve with bovine serum albumin (BSA) dilutions preparations recommended by Bio-Rad using MARS data analysis software (BMG LABTECH GmbH, Ortenberg, Germany)[14].

Protein SDS page

Protein profiles of each stock suspension were analyzed in triplicate by 12% sodium dodecyl sulfate–polyacrylamide gel electrophoresis (SDS-PAGE). The assay was performed to verify the presence and relative abundance of Cry proteins based on their characteristic molecular masses, thereby complementing the total protein quantification obtained by the Bradford assay.Gels (1:10) were stained with 0.05% (wt/vol) Coomassie Brilliant Blue R-250 (Thermo Scientific) in a methanol–acetic acid–water solution (40:10:50, vol/vol/vol). Protein samples were mixed with 4× Laemmli sample buffer, heated at 90 °C for 10 min, cooled on ice for 5 min, and electrophoresed at 120 V. Band densitometric analysis was performed using Phoretix 1D software (TotalLab), with BSA as a reference standard. Protein bands corresponding to the expected molecular masses of Cry1A protoxins (~ 130 kDa), Cry2A protoxins, and Cry1A activated toxins (~ 65 kDa) were detected in all preparations.

Morphological analysis by static image microscopy

The morphological characterisations of all samples (Lip-F, Lip-U, and Delfin®) were performed *ex-situ* using a Morphogranulometer (Morphologi G3S, Malvern Instruments Ltd., Worcestershire UK; serial no.: MAL1033756) operated through Morphologi software v7.21 from the same manufacturer. This optical analysis system, as described, and modified from Barssoum et al.[21], employs a lens system (×1 to ×50 magnification range), and a high-resolution Nikon CFI60 camera (2592 × 1944 pixel, size: 2.7 µm/pixel), enabling accurate imaging-based particle characterisation. In dry-way (DW), and wet-way (WW), the method to extract the statistical measurements were identical to whose previously described[14]. The morphogranulometer system scans, and record images of each identified cell. Additionally, image analysis software called Morphologi v7.21 enabled identifying individual particles as well as determining their geometric properties such as diameter, aspect ratio, circularity, among others. Number, and volume distribution graphs for each parameter were automatically created[22].

Suspendability and sedimentation assessment

The suspendability, and sedimentation of 1 gdm/L suspension (Lip-U, Lip-F, Delfin®) were studied using a Turbiscan LAB™ stability analyser (Microtrac Formulaction SAS, Toulouse, France, measurement range from 0.1 to 1000 µm) based on a multiple light scattering technology. This device can identify and follow the destabilization phenomena (kinetics of particle migration, and size change) of concentrated suspensions in their native state with no additional workup, dilution, or probing. Turbiscan LAB™ is composed of a detection head, which moves up, and down along a flat-bottomed glass cylindrical cell (volume ≈ 20 mL). The detection head is composed of a pulsed near-infrared light source (λ ≈ 880 nm), and two synchronized detectors. The transmission detector (at 180°) receives the light which goes through the sample, while the backscattering detector (45°) receives the light scattered backward by the sample. The detection head scans the entire height of the sample acquiring transmission, and backscattering data at defined intervals of time (2 scans/min). Samples were vortexed for 2 min at maximum speed to standardise initial dispersion then settling, and clarification were monitored during 24 h at 25 °C. Backscattered (BS), and transmitted (T) lights on the y-axis[23] are used to identify particles average diameter (d), and volume fraction (ϕ) as described by Eq. (1), and (2).

$$T\left(d,\Phi_V,\ r_i\right)=T_0\cdot\ Exp\left(-3\cdot\ r_i\cdot\ \Phi_v\cdot\ Q_S\Big/_d\right) \tag{1}$$

$$BS\left(d,\Phi_V\right)=\left(\frac{3.\Phi_V.(1-g).Q_S}{2d}\right)^{1/2} \tag{2}$$

Where *ri* is the inner radius of the measurement cell, Q_s is the scattering efficiency factor, d is the mean particle diameter, Φ_v is the volume fraction of the dispersed phase, and g is the asymmetry factor according to *Mie* theory. Under fixed optical conditions, transmission increases when local particle concentration decreases, whereas backscattering is sensitive to both particle concentration and particle size, making it suitable for following clarification and sediment densification phenomena[24]. Transmission decreases with increasing particle volume fraction due to enhanced light attenuation, whereas backscattering increases with particle concentration and scales as $(\Phi v/d)^{1/2}$. As a result, clarified regions are characterized by high transmission and low backscattering, while sedimented zones exhibit low transmission and high backscattering. Transmission is therefore mainly sensitive to clarification, whereas backscattering reflects both particle accumulation and size-dependent structural changes.

To compare destabilization pathways, three parameters were extracted from the height-resolved backscattering (BS), and transmission (T) profiles over time: (i) the equivalent volume fraction of settling pellet (primary decantation) by integrating ΔBS^2 in bottom-zone backscattered signal (0–4 mm), (ii) the mean volume fraction in supernatant (secondary clarification) through, and the upper-zone transmitted signals (between h = 4 mm, and $0.75h_{max}$, and between $0.75h_{max}$, and h_{max}), and (iii) the clarification kinetics through the width of transmitted signal peak at $\Delta T = 5\%$ over time. These metrics were selected to independently capture sediment build-up kinetics, cumulative sediment densification, and clarification dynamics within the suspension column.

Bioefficacy across multiple pests

The Lip-F formulation was tested, and Delfin® (commercial formulation of *B. thuringiensis* subsp. *kurstaki*) was included as a positive control. At least five concentrations of each product were tested, and treatments were repeated three times. Distilled water was used as a negative control, and mortality in control treatments never exceeded 10%. Bioassays were conducted following species-specific protocols adapted to the biology of each insect.

S. exigua, *O. nubilalis*, and *G. molesta* larvae were obtained from established laboratory colonies at the University of Valencia (Spain). A standard diet surface treatment protocol was applied[25]. Neonate larvae were individually placed in wells of multi-well trays containing artificial diet treated with the corresponding product concentration. Mortality was counted on the 7th day. Each concentration was tested with 16 larvae per repetition.

S. frugiperda larvae were reared on artificial diet at the Julius Kühn Institute (JKI) – Federal Research Centre for Cultivated Plants, Institute for Biological Control (Germany), in a quarantine unit operating under EPPO standards[14]. Each well was filled with 1.5 ml of diet, followed by the addition of 45 µl of the related suspension onto it. For each dilution, and the control, which consisted solely of autoclaved deionized water, one 24-well cell culture plate was created, corresponding to 24 larvae, repeated three times, resulting in a total of 1152 larvae. Bioassays were performed according to the protocol described by Nasreddine et al.[14].

P. absoluta larvae were reared at the Department of Plant Protection, Çukurova University (Türkiye), on potted tomato seedlings maintained at 26 ± 1 °C, 65 ± 5% relative humidity, and a 14:10 h light: dark photoperiod. The bioassay followed the protocol described by Nasreddine et al.[14].

Mortality data from all experiments were analyzed by Probit analysis[26] using POLO-PC software (LeOra Software, Berkeley, CA, USA, 1987). The program provided regression parameters including LC_{50} (the concentration killing 50% of treated individuals), and slope (which indicates the steepness of the dose–response relationship).

Chi-square (χ^2) goodness-of-fit tests implemented in the software were used to determine whether bioassays could be considered statistically similar, and whether slopes were homogeneous. When bioassays were not significantly different, responses were considered equivalent. When bioassays were different, but slopes were parallel, relative potency ratios were calculated across the full dose–response range. When slopes were significantly different, comparisons were based on LC_{50} values and their 95% fiducial limits (FL_{95}), which are considered the most robust parameter for comparing product susceptibility. LC_{50} values were considered not significantly different when their FL_{95} overlapped. If FL_{95} does not overlap, LC_{50} ratios were calculated.

Sunlight simulation assay

Powdered Btk samples (Lip-F, Lip-U, and Delfin®) were dispersed in sterile isotonic saline (0.9% NaCl; 9 g/L, autoclaved) to obtain a stock suspension of 10 mg/mL. Suspensions were homogenized by vortexing, and then mixed on a rotating mixer (continuous 360° rotation, 90 rpm, 10 min). For each product, two sterile frosted glass slides were prepared in parallel, one serving as the non-exposed control, and the other as the exposure sample. Slides were sterilized under sunlight (SL) in a biosafety cabinet for 15 min, after which 500 µL of the corresponding stock suspension was pipetted onto each slide and spread to form a thin film. Slides were dried at 37 °C for approximately 1.5 h until completely dry. Control slides were shielded from light using aluminum foil for the duration of the exposure period, while exposure slides were placed in an Atlas SUNTEST XXL xenon-arc sunlight simulator (Atlas Material Testing Technology LLC, AMETEK, Mount Prospect, IL, USA).

The simulator was operated using irradiance control over 300–800 nm at 350 W/m², with chamber temperature set to 20 °C, and relative humidity to 70%. Cooling and airflow were enabled according to the instrument settings, and samples were exposed for 6 h. After exposure, each slide was transferred into a sterile 50 mL tube, and the dried residue was recovered by rinsing with 5 mL sterile isotonic saline followed by continuous rotation (70 rpm, 15 min). Remaining material was gently detached from the slide using a sterile inoculation loop, slides were removed with sterile forceps, and suspensions were mixed for an additional 1–2 min to standardize recovery. Due to rapid sedimentation of particulate material, suspensions were vortexed immediately prior to each pipetting step.

The same sunlight-exposure workflow, and experimental pairing strategy was applied for CFU enumeration, total protein quantification, and insect bioassays with some modifications based on the experiment.

Repetition-level spore counts were analysed on the $\log_{10}$ CFU ($n = 3$, per treatment). For each product, and repetition, control, and SL-exposed $\log_{10}$ values were paired, and the following quantities were computed:

$$\Delta \log_{10} = \log_{10}(CFU)_{SL} - \log_{10}(CFU)_{Control} \quad (3)$$

$$Rentation\ fraction = \frac{CFU_{SL}}{CFU_{control}} = 10^{\Delta \log_{10}} \quad (4)$$

For total protein concentration the retention percentage was calculated as followed:

$$Retention\,(\%) = 100 \times \frac{SL}{Control} \tag{5}$$

For the *S. frugiperda* bioassays, cumulative deaths were recorded at 24, 48, 72, 96, 120, and 144 h for each repetition ($n = 24$ larvae per repetition, and condition). Mortality curves were visualised as pooled cumulative mortality proportions at each time point, obtained by summing cumulative deaths across replicates, and dividing by the total number of larvae (24 × number of repetitions), and uncertainty around pooled proportions was represented using Wilson 95% binomial confidence intervals. To compare exposed, and non-exposed conditions at the study endpoint (144 h) while controlling for between-replicate variability, a Cochran–Mantel–Haenszel (CMH) test[27] was applied separately for each product using replicate as the stratification factor, yielding a Mantel–Haenszel χ^2 statistic, an associated p-value, and a common odds ratio with 95% confidence interval for the effect of sunlight exposure on mortality calculated as followed:

$$OR = \frac{\left(Dead \middle/ Alive\right)SL}{\left(Dead \middle/ Alive\right)Control} \tag{6}$$

If: OR = 1: no SL effect, OR < 1: SL causes lower mortality and OR > 1: SL causes higher mortality.

In addition, an absolute endpoint effect size was calculated for each repetition as:

$$\Delta_{144} = M_{SL,144} - M_{Control,144} \tag{7}$$

where mortality at 144 h is:

$$M_{SL,144} = \frac{D_{SL,144}}{N}$$

$$M_{Control,144} = \frac{D_{Control,144}}{N}$$

and D is the cumulative number of dead larvae at 144 h, and $N = 24$ larvae per repetition.

Equivalently:

$$\Delta_{144} = \frac{D_{SL,144} - D_{Control,144}}{N} \tag{8}$$

The entire analysis, and visualization tasks were performed in R software version 4.4.0 (R Core Team, 2025) from the stats package *stats: mantelhaen.test()* for CMH testing, and the *binom* package for Wilson confidence intervals, data handling, and plotting were conducted with *dplyr*, and *ggplot2*[28,29]. Median lethal time (LT_{50}) was estimated as the time required to achieve 50% cumulative mortality, using linear interpolation between observation intervals, consistent with classical time–mortality analysis described by Preisler & Robertson[30].

Results

Physicochemical parameters, spores, and proteins concentrations during culture

Culture behaviours were reproductible ($n = 4$) as demonstrated by the mean evolution of physicochemical parameters and monitored over 72 h for all phases (Fig. 2A). Temperature (30 °C), pH (6.8-7), agitation (600 rpm/10 rps), and aeration (1.6 nL/min) were accurately regulated. Dissolved oxygen concentration (pO_2) exhibited a marked temporal variation with a significant and expected standard deviation during the main culture phases. High pO_2 values were recorded at the start of fermentation, followed by a rapid decrease during the first 10 h (oxidative growth). Thereafter, pO_2 progressively increased, and stabilized during the mid-fermentation period (30 h) before rising further toward the end of the process informing about nutritional limitation/sporulation, and lysis respectively.

The respiratory activity, derived from gas balance (Fig. 2B), indicated a transition from an initial growth-associated high respiratory activity to a prolonged low-respiration regime accompanying sporulation, and coincided with the increase in spore concentration (Fig. 3), in agreement with the online physicochemical trends (Fig. 2A). During the first 10 h, r_{CO2} (volumetric CO_2 evolution) increased rapidly to a distinct maximum, while r_{O2} (volumetric O_2 uptake) showed the highest oxygen demand, consistent with intense oxidative metabolism during exponential cell biomass growth. Concomitantly, dissolved oxygen (pO_2) decreased sharply from near saturation to a minimum (Fig. 2A), indicating a transient oxygen transfer limitation during peak respiration. After 10 h, r_{CO2} progressively declined, and r_{O2} moved toward lower absolute uptake, reflecting a reduction in global respiratory activity as growth decelerated, and the culture transitioned into stationary phase. In parallel, pO_2 steadily recovered (Fig. 2A), consistent with a decreasing oxygen demand, and restoration of a positive oxygen transfer margin under otherwise stable operating conditions (constant agitation, aeration, pH, and temperature).

Between 10 and 45 h, the respiratory quotient ($RQ = r_{CO2}/r_{O2}$) increased, and remained elevated as shown in Fig. 2B. This period coincided with the pronounced increase in spore concentration shown in Fig. 3, was therefore consistent with the transition from vegetative growth to sporulation-associated physiology. From 45 h onward, r_{CO2} stabilized at a comparatively low level with a modest secondary increase around 50–60 h, whereas r_{O2} remained low, suggesting residual maintenance metabolism and potentially the utilization of remaining substrates during the late phase. Notably, short-lived RQ excursions occurred at discrete time points (e.g., 30–

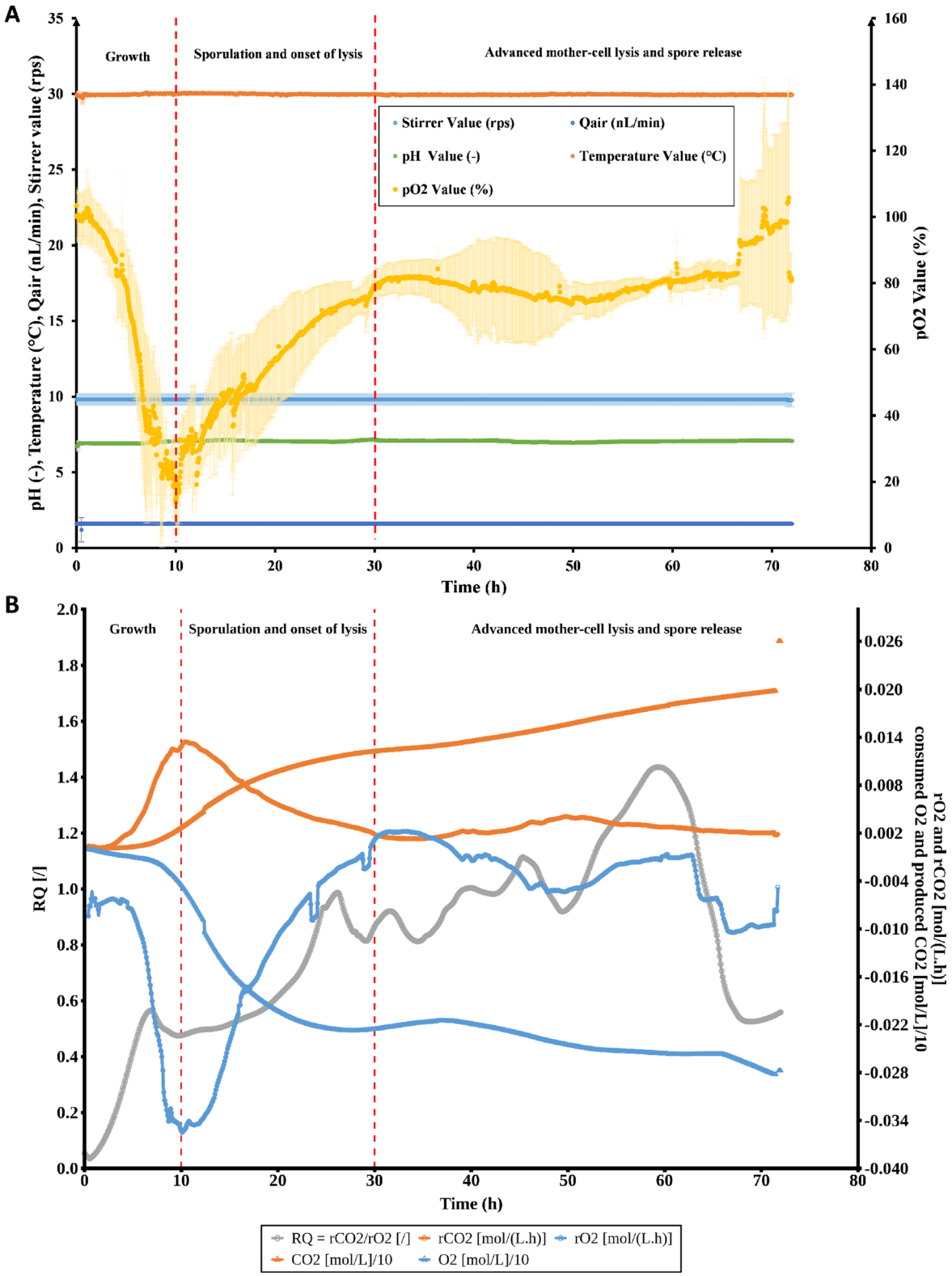


Fig. 2. Evolution of bioreactor process variables and respiratory activity versus time. (**A**) Mean ± SD ($n = 4$) profiles of impeller speed (rps), aeration rate (Qair, nL/min), pH, temperature (°C), and dissolved oxygen (pO_2, % air saturation) over 72 h. (**B**) Off-gas respiratory profile ($n = 4$) showing volumetric oxygen uptake (rO_2V, mol/L·h), carbon dioxide evolution (rCO_2V, mol/L·h), the respiratory quotient ($RQ = rCO_2V/rO_2V$, dimensionless), and scaled cumulative consumed O_2 and produced CO_2.

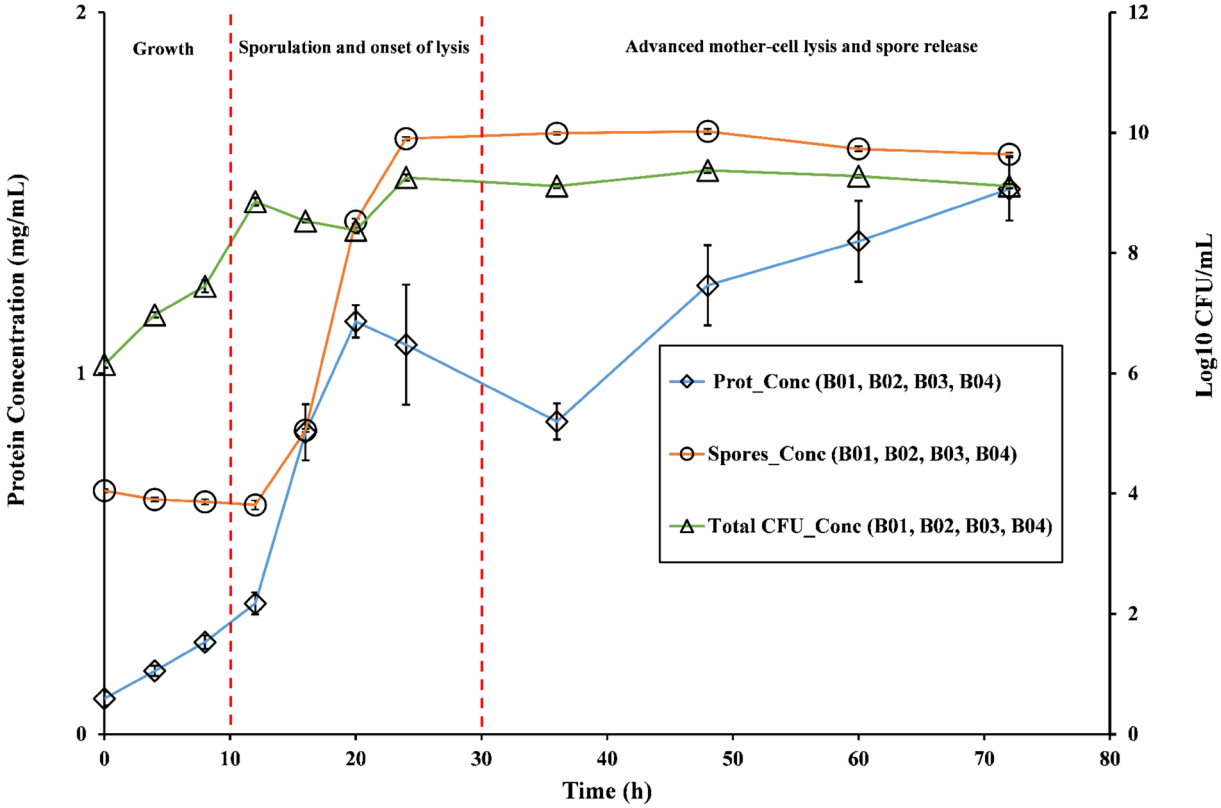


Fig. 3. Evolution of protein (mg/mL), total count and spore concentration (log_{10} CFU/mL) during cultures ($n = 4$), mean values, and error bars indicate standard deviation of the mean).

40 h, and later in the run), which coincide with near-zero and therefore should be interpreted cautiously due to ratio instability rather than as true metabolic transitions.

These respiratory dynamics coincided with the kinetics of protein accumulation, and spore formation (Fig. 3). During the early phase (0–12 h), protein concentrations increased gradually (0.15 to 0.35–0.4 mg/mL) while spore counts remained low (4.5–5.0 log_{10} CFU/mL). A pronounced increase in both parameters occurred between 12 and 24 h, with protein concentrations reaching 1.1–1.2 mg/mL, and spore counts rising sharply to 9.0–9.5 log_{10} CFU/mL, consistent with the onset, and progression of sporulation during the period of declining respiratory activity and recovering pO_2.

From 24 h onward, spore concentrations remained high, and relatively stable, close to 9.5–10.0 log_{10} CFU/mL, whereas protein concentration continued to increase, reaching final values of approximately 1.4–1.5 mg/mL at 72 h. This late phase coincided with increasing pO_2 levels and reduced respiratory activity, consistent with a late stationary or post-sporulation phase. As the Bradford assay quantifies total solubilized protein, the observed increase was not interpreted as a direct measure of Cry-protein production. SDS-PAGE confirmed the presence of bands in the formulation phase at the expected molecular masses of major Cry proteins in the analysed preparations but was not used for time-resolved quantification of Cry synthesis.

Physical properties of formulations, and suspensions

Particle size, and shape were quantified using both number-based (En), and volume-based (Ev) morpho-granulometric descriptors for Lip-U, Lip-F, and Delfin[*][14], under dry-way (DW), and wet-way (WW) conditions (Table 1).

Under DW, Lip-U, and Lip-F displayed comparable number distributions, with median diameters ($D_{n-0.5}$) of 10.23, and 10.94 µm, respectively, and similar upper percentiles ($D_{n-0.9}$ = 21.3 µm for both). Lip-U, and Lip-F number-weighted mean diameters (D[1,0]) were 12.02 ± 7.16 µm, and 12.43 ± 7.39 µm, with mean aspect ratios, AR of 0.78 ± 0.14, and 0.81 ± 0.13, and high-sensitivity circularity, HSCir of 0.87, and 0.90, respectively. On a number basis, the fine fraction < 5 µm represented 12.01% (Lip-U), and 10.67% (Lip-F), whereas particles > 30 µm accounted for 2.38%, and 2.20%, and > 100 µm for 0.04%, and 0.10%, respectively. Delfin[*] showed a coarser number distribution ($D_{0.5}$ = 17.57 µm; $D_{0.9}$ = 54.92 µm; D[1,0] = 28.78 ± 41.46 µm) with a higher proportion of particles > 30 µm (24.53%). In contrast, volume distributions revealed pronounced differences in the coarse tail. Lip-U showed $D_{V-0.5}$ = 24.93 µm, and D[4,3] = 44.27 ± 68.01 µm, with 35.3% of volume > 30 µm, and 8.5% >100 µm. Lip-F exhibited a markedly extended coarse fraction ($D_{v-0,0.9}$ = 1269 µm; D[4,3] = 328.2 ± 463.4 µm),

		$D_{n-0.1}$	$D_{n-0.5}$	$D_{n-0.9}$	D[1,0] ±SD	AR ±SD	HSCir ±SD	Fine, and Coarse [%]		
								< 5 µm	> 30 µm	> 100 µm
Number distribution										
Dry way (DW)	Lip-U	4.77	10.23	21.32	12.02 ± 7.16	0.78 ± 0.14	0.87 ± 0.13	12.01	2.38	0.04
	Lip-F	4.92	10.94	21.31	12.43 ± 7.39	0.81 ± 0.13	0.90 ± 0.11	10.67	2.20	0.10
	Delfin*	5.64	17.57	54.92	28.78 ± 41.46	0.78 ± 0.14	0.86 ± 0.14	8.32	24.53	3.13
Wet way (WW)	Lip-U	0.62	0.93	1.64	1.35 ± 2.00	0.83 ± 0.15	0.81 ± 0.15	96.87	0.04	0.04
	Lip-F	0.62	0.98	1.67	1.32 ± 1.55	0.82 ± 0.16	0.80 ± 0.15	97.54	0.06	0.06
	Delfin*	0.94	1.77	2.30	1.78 ± 1.04	0.80 ± 0.14	0.83 ± 0.16	99.39	0.23	0.23

		$D_{v-0.1}$	$D_{v-0.5}$	$D_{v-0.9}$	D[4,3] ±SD	AR ± SD	HSCir ±SD	Fine, and Coarse [%]		
								< 5 µm	> 30 µm	> 100 µm
Volume distribution										
Dry way (DW)	Lip-U	12.9	24.9	59.2	44.3 ± 68.0	0.84 ± 0.14	0.91 ± 0.13	0.19	35.27	8.53
	Lip-F	14.9	36.0	1269.0	328.2 ± 463.4	0.86 ± 0.13	0.93 ± 0.11	0.10	57.04	39.37
	Delfin*	127.0	326.8	873.3	382.2 ± 240.9	0.91 ± 0.14	0.91 ± 0.14	0	99.28	93.07
Wet way (WW)	Lip-U	8.77	20.56	36.04	21.8 ± 10.5	0.88 ± 0.15	0.87 ± 0.15	3.47	20.75	0
	Lip-F	8.20	19.21	37.40	21.5 ± 34.2	0.88 ± 0.16	0.87 ± 0.15	4.54	19.31	0
	Delfin*	2.08	35.48	124.30	52.4 ± 45.1	0.85 ± 0.14	0.89 ± 0.16	18.95	54.09	21.73

Table 1. Morpho-granulometric parameters of the Lip formulations obtained by dry-way (DW), and wet-way (WW) processing. Delfin* data was extracted from Nasreddine et al. [14]. Particle size distributions are expressed on a number (En), and volume (Ev) basis. $D_{0.1}$, $D_{0.5}$, and $D_{0.9}$ correspond to the 10th, 50th, and 90th percentiles, respectively. D[1,0] and D[4,3] represent the surface and volume-weighted mean diameters (mean ± SD). Aspect ratio (AR), and high-sensitivity circularity (HS Cir) describe particle shape characteristics. Coarse fractions are reported as the percentage of particles below 5 µm, and above 30 µm, and 100 µm, calculated on a number- or volume-basis as indicated. Composite images were added to supplementary data.

with 57.04% of volume > 30 µm, and 39.4% >100 µm. Delfin* showed similarly coarse volume characteristics (D[4,3] = 382.2 ± 239.9 µm), with 99.3% >30 µm, and 93.1% >100 µm.

Under WW, Lip-U, and Lip-F shifted to submicron number distributions ($D_{n-0.5}$ = 0.93, and 0.98 µm; $D_{n-0.9}$ = 1.64, and 1.67 µm; D[1,0] = 1.35 ± 2.00, and 1.32 ± 1.55 µm), with high fine fractions < 5 µm (96.9%, and 97.5%), and negligible number fractions > 30 µm (≤ 0.06%). Delfin* also showed a fine number distribution ($D_{n-0.5}$ = 1.77 µm) with 99.4% <5 µm. In volume distributions, Lip-U, and Lip-F remained centered at 20–21 µm (D[4,3] = 21.8 ± 10.5, and 21.5 ± 34.2 µm) with no detectable volume fraction > 100 µm, while Delfin* retained a larger coarse contribution (D[4,3] = 52.4 ± 45.1 µm) with 21.7% of volume > 100 µm.

Representative Morphologi G3S composite images qualitatively supported the granulometric distributions (Fig. 4). Under dry-way conditions, Lip-U and Lip-F were dominated numerically by smaller particles, whereas Delfin* showed a visibly greater occurrence of coarse particles (Fig. 4A–C). Following wet dispersion, all formulations were dominated by fine particles on a number basis; however, Delfin* retained visibly larger residual structures, consistent with its greater coarse contribution in the volume-weighted distribution (Fig. 4D–F).

Physical suspendability of suspensions was monitored through the analysis of backscattered, and transmitted signals over time, and height. Changes in transmission ($\Delta T = T(t) - T(t_0)$), and backscattering ($\Delta BS = BS(t) - BS(t_0)$) light were used to track a primary sedimentation, and a secondary clarification with comparisons based on relative trends, and kinetics under identical optical conditions (Fig. 5).

Suspension destabilization was resolved into bottom sediment build-up and supernatant clarification using integrated bottom backscattering and transmission-derived concentration profiles (Fig. 6A). Lip-U, used as the unformulated baseline, showed the strongest increase in the integrated bottom signal over time, indicating the highest extent of particle accumulation in the lower zone [0–4 mm]. Lip-F displayed a reduced bottom build-up relative to Lip-U throughout the experiment, whereas Delfin* showed the lowest values overall. For all three suspensions, the increase was steepest during the first hours and then progressively slowed, approaching a plateau-like behaviour after approximately 20 h.

The transmission-derived concentration proxy, expressed as *ln(T0) – ln(T)*, showed different spatial patterns depending on the height zone considered. In the bulk region [4 mm–0.75·h_max], Delfin* exhibited a more

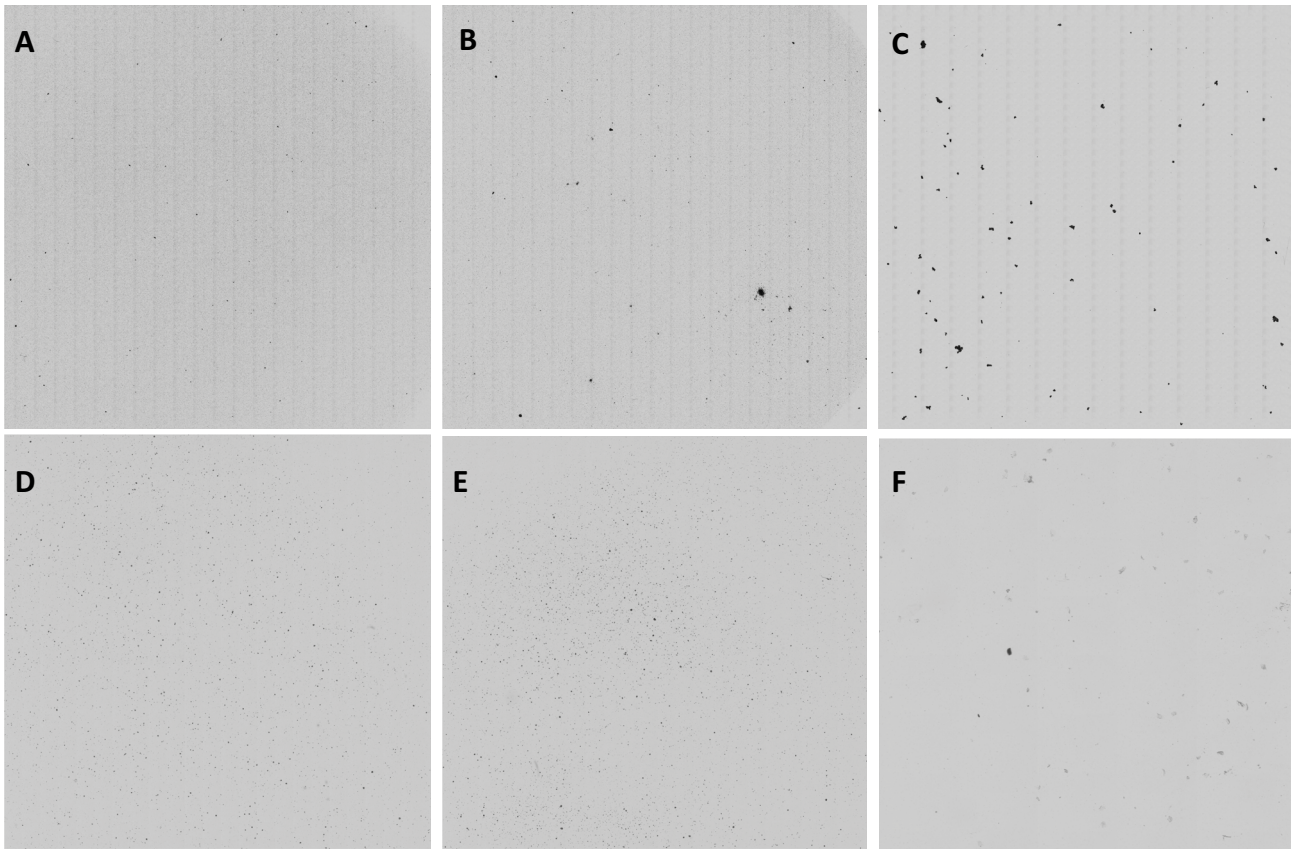


Fig. 4. Representative composite Morphologi G3S images of the formulations acquired at 2.5× magnification under dry-way (DW) and wet-way (WW) conditions. Panels **A**–**C** show Lip-U (**A**), Lip-F (**B**), and Delfin® (**C**) under DW conditions, while panels **D**–**F** show Lip-U (**D**), Lip-F (**E**), and Delfin® (**F**) under WW conditions. Images were obtained using the ScanAreaComposite function and are presented as representative visual support for the morpho-granulometric analysis, illustrating differences in particle abundance, dispersion, and the occurrence of coarse particles/agglomerates among formulations and between dry and wet measurement modes.

progressive and continuous change over time, whereas Lip-F remained lower and Lip-U showed the weakest evolution. In the upper zone [0.75·h_max–h_max], all suspensions showed a decrease in $ln(T0) - ln(T)$, consistent with particle depletion and development of a clarified supernatant layer. This decrease occurred earliest for Delfin®, while Lip-F showed a delayed but marked upper-zone evolution relative to the Lip-U baseline. Lip-U displayed the slowest and least pronounced change in the upper region. Taken together, the profiles indicate that Delfin® underwent the earliest clarification over the suspension height, Lip-F showed an intermediate behaviour, and Lip-U remained the most delayed system.

Clarification kinetics were further quantified from the displacement of the clarification front at a fixed transmission threshold (ΔTR = 5%) (Fig. 6B). A linear relationship between front displacement (Δh) and time was obtained for both Lip-F and Lip-U during the main clarification phase. This approach was applicable to Lip-F and Lip-U, which exhibited a front-like secondary clarification behaviour, allowing linear tracking of Δh over time. In contrast, Delfin® displayed a more homogeneous clarification over the liquid height and therefore did not present a clearly defined moving front suitable for this analysis. The slope of the regression line was higher for Lip-F (0.49 mm/h, $R^2 = 0.99$) than for Lip-U (0.38 mm/h, $R^2 = 0.99$), indicating faster front propagation in the formulated suspension than in the unformulated baseline.

The biological performance of Lip-F therefore cannot be attributed to particle size or sedimentation behaviour alone. Instead, it may reflect the combined contribution of the formulation matrix, preservation of the active biological material, particle architecture after reconstitution, and suspension behaviour. The present experimental design did not isolate the independent contribution of each physicochemical parameter to efficacy.

Quality control, and toxicity tests

Quality control was performed to ensure the consistency, biological integrity, and performance of the formulated Bt product prior to bio-efficacy evaluation. Quantification of total, and heat-resistant spores was used to verify spore yield, and stability, which are critical parameters for product potency and shelf life. Total protein determination provided an overall measure of toxin-associated protein content and batch-to-batch consistency. SDS–PAGE analysis was conducted to confirm the presence and integrity of the characteristic Cry

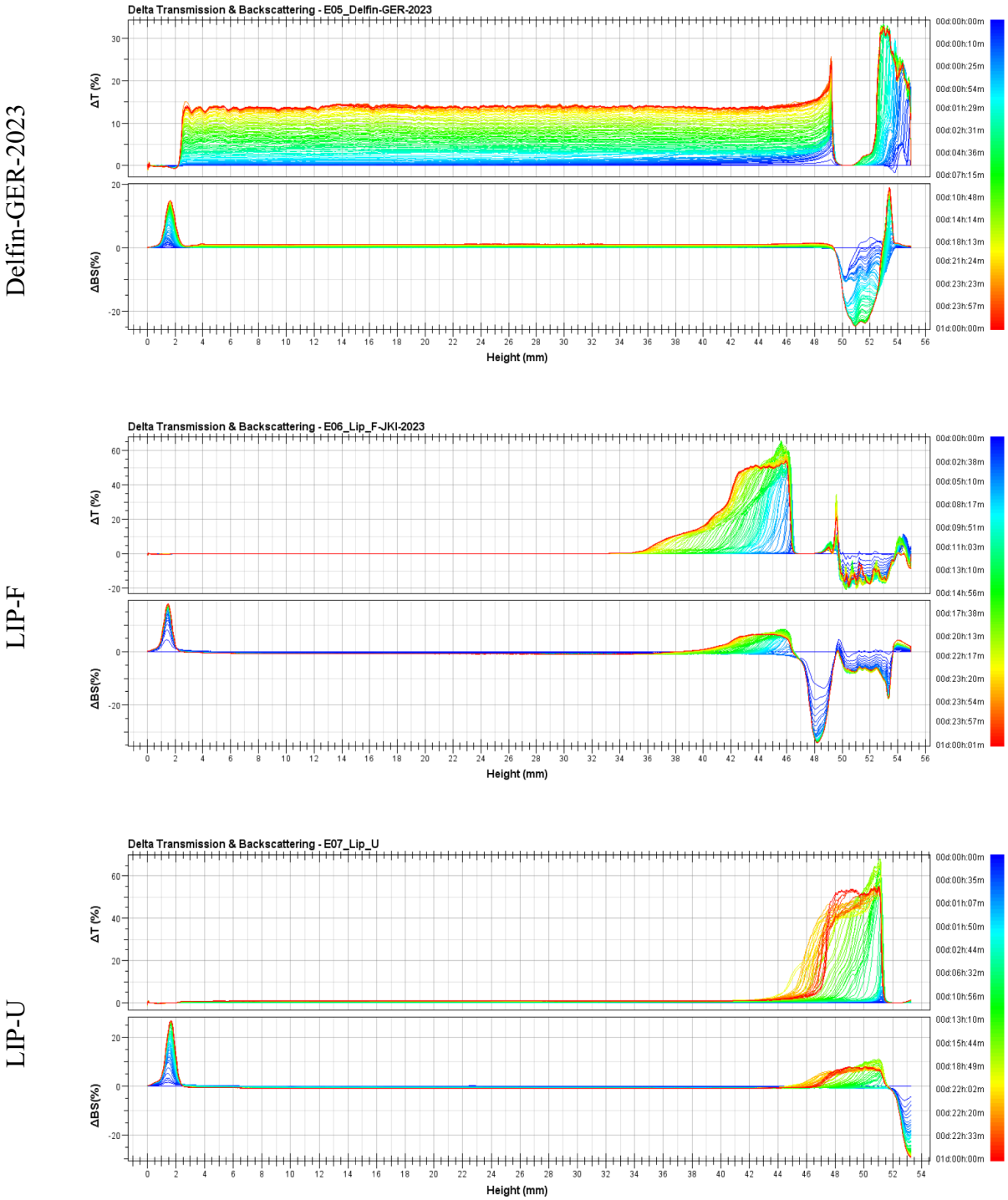


Fig. 5. Evolution of relative Transmitted, ΔT = T(t)-T(t = 0), and Backscattered, ΔBS = BS(t)-BS(t = 0), signals as a function of suspension height (from 0 up to 46/52 mm), and time (< 24 h) for Delfin-GER-2023(Delfin®), Lip-F, and Lip-U suspensions (1 g/L) under static condition at 25 °C. The marked zone, and arrows in red defines the specific analysed zones.

protein profiles, and to detect potential protein degradation or loss during processing. Finally, LC_{50} bioassays against multiple target pests were carried out to link physico-chemical, and biochemical quality attributes with functional insecticidal efficacy. Together, these complementary analyses provide a robust framework for assessing formulation quality before comparative, and field evaluations.

Spore concentration, qualification, and quantification of proteins

Total viable cell counts, heat-resistant cell counts, and total protein content were quantified for the Lip-F formulation, and compared with the commercial reference Delfin® (Table 2). CFU values were comparable among samples for both total cells, and spores. Spore counts were approximately one order of magnitude lower than total cell counts, suggesting that only a small fraction of the cells present in the products corresponded to viable cells.

Cry proteins purified from the samples were analyzed by SDS-PAGE (Fig. 7), revealing the typical profile with two major bands of approximately 130 kDa, and 60–65 kDa, corresponding to the protoxin, and activated toxin forms of Cry1A, and Cry2A proteins, respectively, whose genes are present in the strain[15].

Retention of spores, and total proteins after sunlight exposure

Spore viability, expressed as $\log_{10}$ CFU/g, was quantified for each product under control conditions, and after sunlight exposure across three independent repetitions. For each repetition, paired control, and SL-exposed values were used to calculate $\Delta\log_{10}$(SL − control), the corresponding log reduction, and retention (%).

At the repetitions level, Lip-U control values were 9.23, 9.18, and 8.78 $\log_{10}$ CFU/g, while SL-exposed values were 7.60, 7.61, and 6.48 $\log_{10}$ CFU/g, yielding $\Delta\log_{10}$ values of − 1.63, − 1.57, and − 2.30, and retention values of 2.34%, 2.69%, and 0.501%, respectively. Lip-F control values were 8.61, 8.58, and 8.80 $\log_{10}$ CFU/g, while SL-exposed values were 8.07, 8.13, and 8.18 $\log_{10}$ CFU/g, yielding $\Delta\log_{10}$ values of − 0.540, − 0.450, and − 0.620, and retention values of 28.8%, 35.5%, and 24.0%, respectively.

When results were summarised by product (mean ± SD; $n = 3$), the mean $\Delta\log_{10}$ (SL − control), mean log reduction (control − SL), and mean CFU retention (%) were calculated. Lip-U exhibited a mean log reduction of 1.83 ± 0.41, corresponding to a mean CFU retention of 1.85 ± 1.18%. In contrast, Lip-F showed a substantially lower mean log reduction of 0.54 ± 0.09, corresponding to a mean CFU retention of 29.4 ± 5.89%.

The mean $\log_{10}$ reduction observed for Lip-F was significantly lower than that of Lip-U (t-test, $p < 0.05$), corresponding to a reduction difference of approximately 1.3 log units.

For total protein measured by Bradford assay, mean values (mg/g) decreased from 112.37 to 69.76 for Lip-U, corresponding to a 62.1% protein retention after exposure,, and from 104.25 to 84.43 for Lip-F, corresponding to an 81.0% protein retention. Cry toxin integrity was assessed via SDS-PAGE after sunlight exposure (Fig. 6). Results showed a remarkable degradation for Lip-U, in comparison with Lip-F.

Toxicity analysis

Bioassays of five lepidopteran pests The formulations were toxicologically evaluated against five lepidopteran species from different clades, including two species of the genus *Spodoptera* (*S. frugiperda*, and *S. exigua*). Mortality data were analysed by Probit analysis to estimate LC_{50} values, and slope parameters (Table 3).

Because bioassay protocols differed across species, direct comparisons of LC_{50} values are not appropriate. Therefore, comparisons were restricted to different products within the same insect species. All products showed increasing mortality with increasing concentration, with comparable slope values. Moreover, for *S. frugiperda* ($\chi^2 = 2.8$, df = 2, $p = 0.25$), and *P. absoluta* ($\chi^2 = 1.8$, df = 2, $p = 0.40$), the equality test of Probit lines indicated no significant differences among treatments (supplementary table). In addition, LC_{50} values showed overlapping FL_{95} intervals, confirming similar toxicity across products for these species.

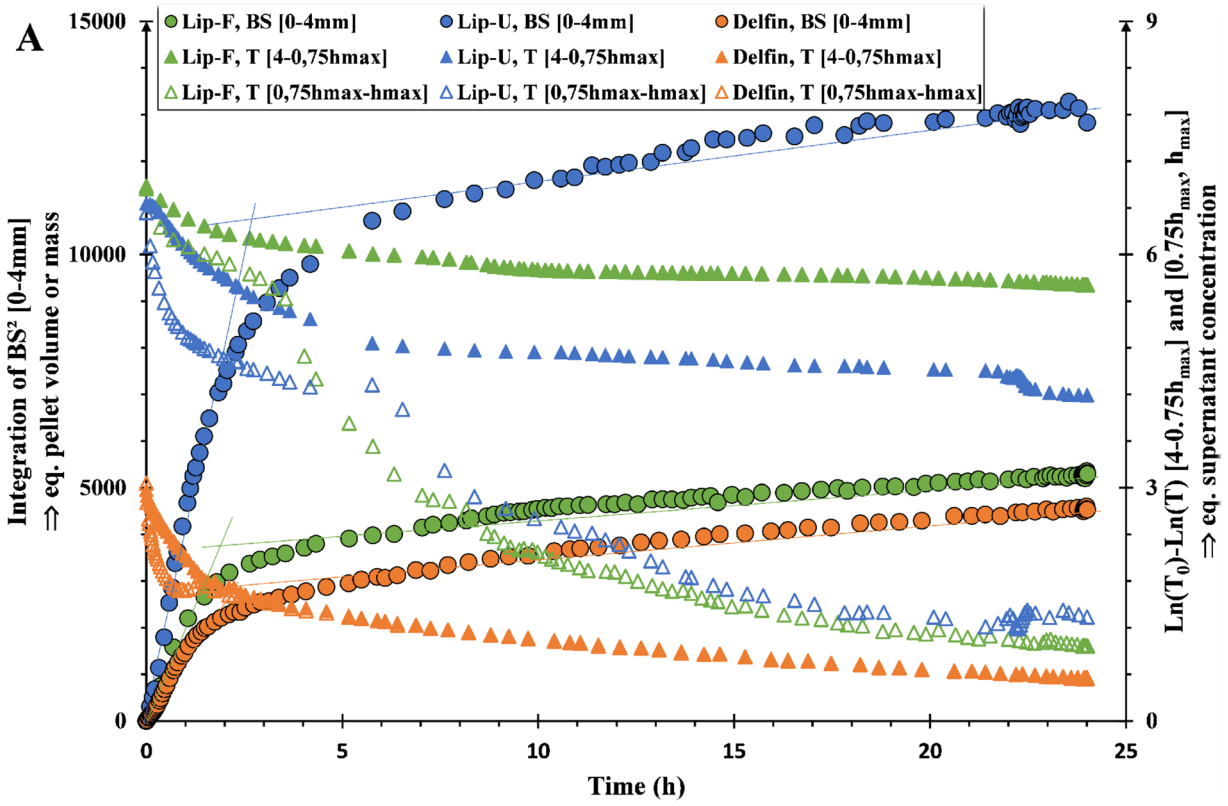
Bioassays with *S. frugiperda* under sunlight stimulator stress Same experimental design of the bioassay was used. Across the observation window, mortality increased rapidly in the non-exposed controls for both products, whereas sunlight-exposed samples showed reduced killing, most prominently for the unformulated biomass (Lip-U) (Fig. 8). At 144 h, the Cochran–Mantel–Haenszel (CMH) test stratified by reptations confirmed a strong exposure effect for Lip-U (Mantel–Haenszel $\chi^2 = 65$, df = 1, $p = 5 \times 10^{-16}$), with a common odds ratio (SL vs. control) of 0.038 ($CI_{95\%}$: 0.015–0.098), indicating markedly lower odds of death after exposure. For the formulated product (Lip-F), the exposure effect was smaller but remained significant (Mantel–Haenszel $\chi^2 = 4$, df = 1, $p = 0.029$), with a common odds ratio of 0.217 ($CI_{95\%}$: 0.058–0.809).

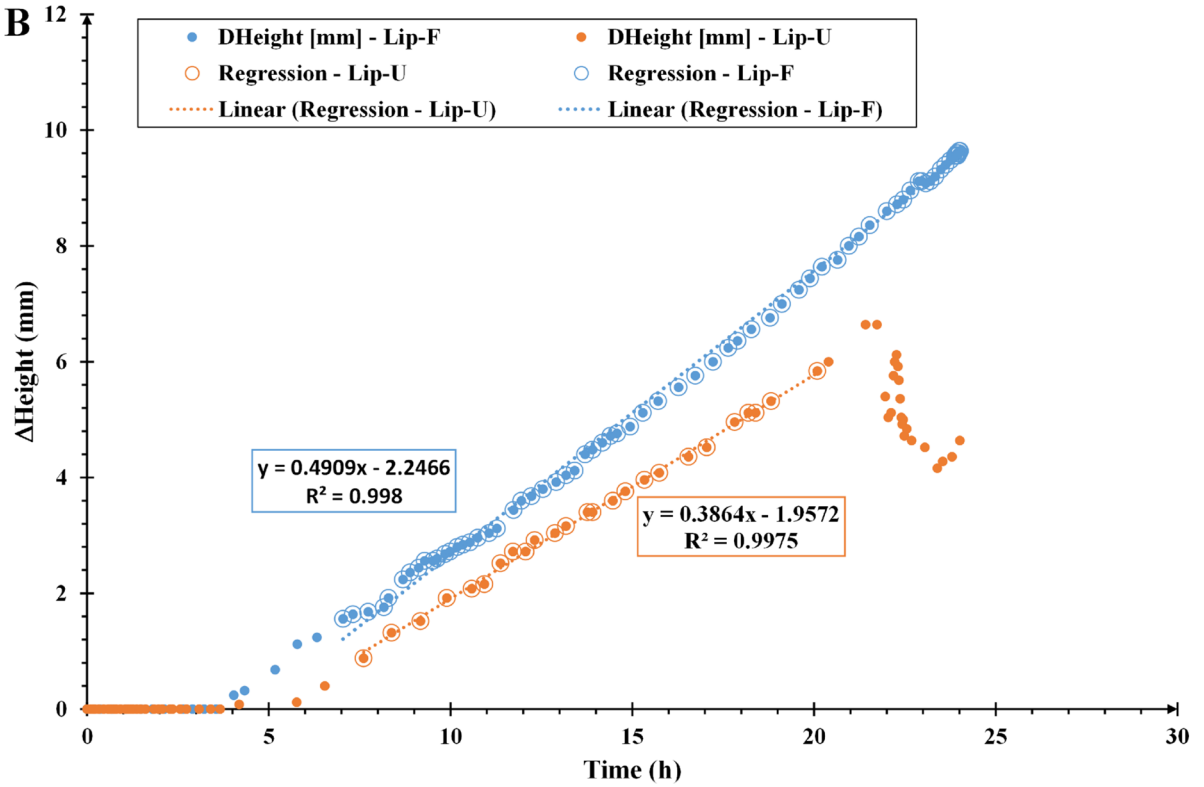
Consistent with the CMH analysis, repetition-wise endpoint effect sizes showed that exposure reduced final mortality (144 h) by − 0.573 ± 0.063 (mean ± SD of Δ[SL − control]) for Lip-U, compared with − 0.094 ± 0.099 for Lip-F. Time-to-effect analysis further supported these trends, LT_{50} for Lip-U controls was 24.8 ± 8.42 h, while LT_{50} for exposed Lip-U was not reached within 144 h in all repetitions. For Lip-F, LT_{50} increased from 21.7 ± 7.91 h (control) to 33.0 ± 19.2 h (exposed), indicating a moderate delay in mortality following exposure.

The mortality curves show that sunlight exposure reduced killing for both products, but the magnitude differed strongly between formulations. For Lip-U, sunlight exposure caused a pronounced, and persistent loss of efficacy, with mortality remaining low throughout the assay, and reaching only 33–38% at 144 h, compared with 88–100% in the paired controls. This matches the endpoint statistics, where the exposure effect at 144 h was large (common OR 0.038, $CI_{95\%}$: 0.015–0.098), and the absolute endpoint change was substantial (Δ[SL − control] − 0.573 ± 0.063). In contrast, Lip-F retained high bioactivity after exposure where mortality under sunlight exposure rose to 83–100% by 144 h, and remained close to the control trajectory, consistent with a smaller exposure effect (common OR 0.217, $CI_{95\%}$: 0.058–0.80), and a modest mean endpoint decrease (Δ[SL − control] − 0.094 ± 0.099).

Discussion

Across the four independent cultures, the coherent evolutions of pO_2, r_{CO2}, and r_{O2} confirm a classical Bt growth trajectory characterized by an initial oxidative growth phase followed by a nutritional-limited transition into stationary phase, and sporulation. In our tightly controlled 72 h cultures, Btk Lip followed the expected pattern of rapid growth followed by sporulation. During the first 10 h the culture showed a sharp decline in pO_2, and





a spike in CO_2 emission, reflecting an intense aerobic growth phase. Such high-respiration conditions support rapid biomass accumulation and can contribute to high final spore yields. In a study, Boniolo et al.[31] found that maintaining pO2 at 50% drastically increased biomass, and spore production. In our runs, the later decline in CO_2 output, and recovery of pO_2 coincided with nutrient exhaustion, and the on-set of stationary phase, consistent with the well-known trigger of sporulation by nutrient depletion[32]. This sequence of vigorous early respiration followed by declining metabolic activity aligns with established Bt kinetics and demonstrates that the controlled process reproducibly captured the transition from vegetative growth to sporulation. Notably, we observed transient artifacts in the respiratory quotient (RQ) whenever r_{O2} or r_{CO2} approached zero (e.g. at very

◂**Fig. 6**. Evolution of backscattering and transmission signals during the sedimentation of Lip-F, Lip-U and Delfin® formulation suspensions. **(A)** Changes in the integrated squared backscattering signal (BS2) within the bottom 0–4 mm of the sample, used as an indicator of sediment accumulation (circles; left axis), and changes in the logarithmic transmission signal [$\ln(T_0) - \ln(T)$], reflecting variations in particle concentration (triangles; right axis). Filled and open triangles represent transmission measurements in the upper (4 mm to 0.75hmax) and lower (0.75hmax to hmax) regions, respectively. Green, blue and orange symbols correspond to Lip-F, Lip-U and Delfin®, respectively. **(B)** Evolution of the transmission peak width (Δh, mm) over time at a constant transmission threshold (ΔTR = 5%) for Lip-F (blue) and Lip-U (orange). Dotted lines represent linear regressions, with the corresponding equations and coefficients of determination (R2) indicated in the graph.

Formulations	Total cells (log_{10} CFU/g)	Spores (log_{10} CFU/g)	Total protein (mg/g)	Cry proteins (mg/g)
Lip-F	14.27 ± 0.03	12.94 ± 1.85	104.24 ±15.41	4.95 ± 1.48
Delfin®	14.16 ± 0.02	12.85 ± 2.32	60.77 ±12.98	4.14 ± 0.69

Table 2. Estimation of total viable cells, spore counts, and total protein content (Bradford assay) in each sample. Additional quantification of Cry protein content (mg/g) was performed by densitometric analysis of the ≈ 65 kDa, and ≈ 130 kDa bands obtained from SDS-PAGE. Microbial counts were log_{10}-transformed prior to statistical analysis. Cell counts are presented as log_{10} CFU/g of formulation, and protein content as mg protein/g of formulation. For protein concentration, determined by the Bradford assay, was 104.24 mg/g for Lip-F, and 61 mg/g for Delfin® which is significantly lower than the Lip-based formulations (t-test, $p < 0.05$).

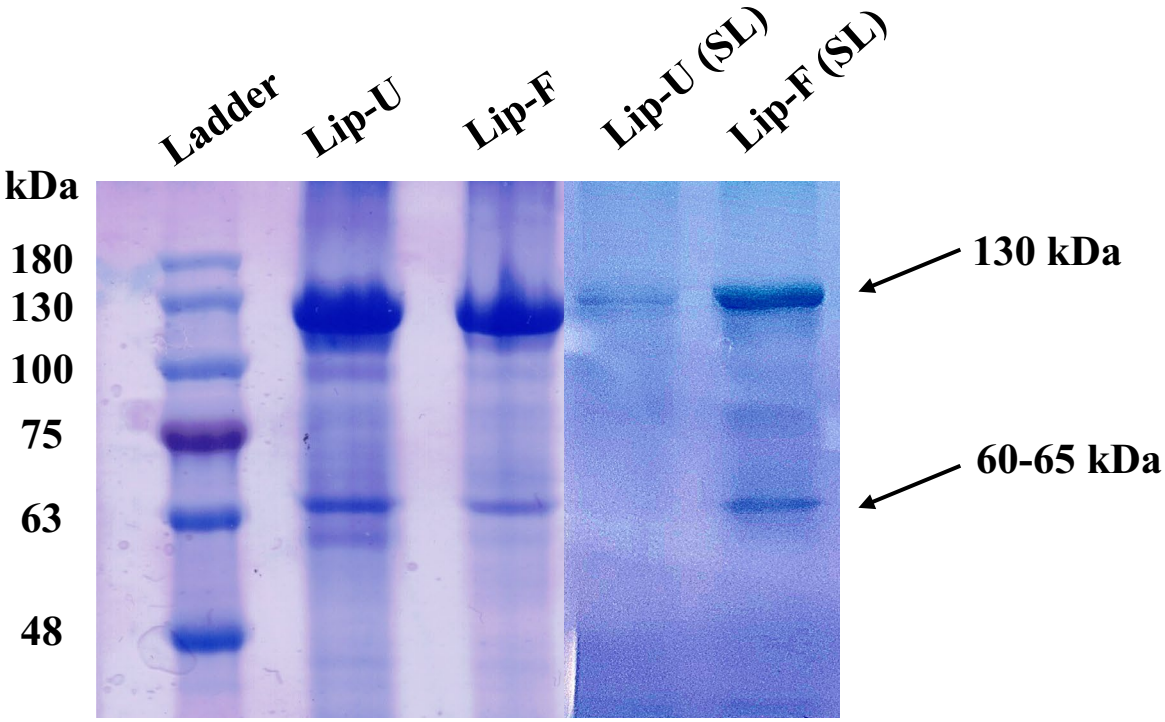


Fig. 7. Protein analysis of the samples by 12% SDS-PAGE. Gels were stained with Coomassie Brilliant Blue. BSA (mg/g) was used as a standard to estimate protein concentration (supplementary data). Ladder: molecular weight marker 10–180 kDa (BlueStar Pre-stained Protein Ladder, Nippon Genetics, Lip-U: unformulated material as reference, Lip-F: formulated product from Lip strain. Arrows indicate the expected activated toxin, and protoxin forms of Cry1A, and Cry2A proteins. After sunlight exposure, the profile of Lip-U, and Lip-F is also presented. (Full gel presented supplementary data)

early [< 5 h] or late times [40 h] when the calculated respiratory rates approached zero). These near-zero values are often due to analyser limits rather than biology, so those periods were filtered in analysis.

The cultures used a WB complex medium, an agro-industrial by-product chosen for cost-effectiveness[33]. WBsupplies a mix of carbohydrates, proteins, and minerals, and has been shown to support robust Bt growth, and δ-endotoxin production. Its composition, however, contains only 3% protein-bound nitrogen[21], so nitrogen

Species	Treatments	LC_{50} (ng/cm²)	FL_{95}	Slope
S. frugiperda	Lip-F	8308	6479–10,652	1.8 ±0.2
	Delfin®	11,071	3773–21,714	2.2 ±0.3
S. exigua	Lip-F	138	23–436	1.2 ±0.2
	Delfin®	271	176–681	1.8 ±0.3
P. absoluta	Lip-F	3929	1390–6400	3.1 ±0.5
	Delfin®	3301	1476–4916	3.3 ±0.5
G. molesta	Lip-F	2.5	0.3–5.4	1.4 ±0.2
	Delfin®	11	0.8–35	1.0 ±0.1
O. nubilalis	Lip-F	2.8	1.0-4.3	1.3 ±0.2
	Delfin®	6.5	4.3-9	1.4 ±0.2

Table 3. Susceptibility of five lepidopteran pests to Lip-F, and Delfin® in laboratory bioassays. Each insect species was subjected, in triplicate, to a bioassay protocol adapted to its biology. Parameters were estimated by Probit analysis. LC_{50}: concentration causing 50% mortality of treated individuals. FL95: lower, and upper 95% fiducial limits of the LC_{50} value. Slope: slope of the regression line of log(dose) versus mortality, with its standard error. LC_{50} values were considered significantly different when their FL_{95} did not overlap. Statistical analysis of slope homogeneity (parallelism test) is presented as supplementary data. LC_{50} values revealed no significant differences between Lip-F, and Delfin® in any species except *O. nubilalis*, where Lip-F showed greater activity (LC_{50} ratio = 2.3). Slopes were not significantly different (parallelism test, $p > 0.05$), indicating parallel dose–response curves. However, the equality test of Probit lines showed a significant difference ($\chi^2 = 7.3$, df = 2, $p = 0.03$), demonstrating a displacement between regression lines, and therefore a difference in potency. The relative potency of Lip-F across the full bioassay range was 2.2-fold higher than Delfin® (FL_{95} = 1.2–3.9). Overall, these results indicate comparable performance between both products across most species.

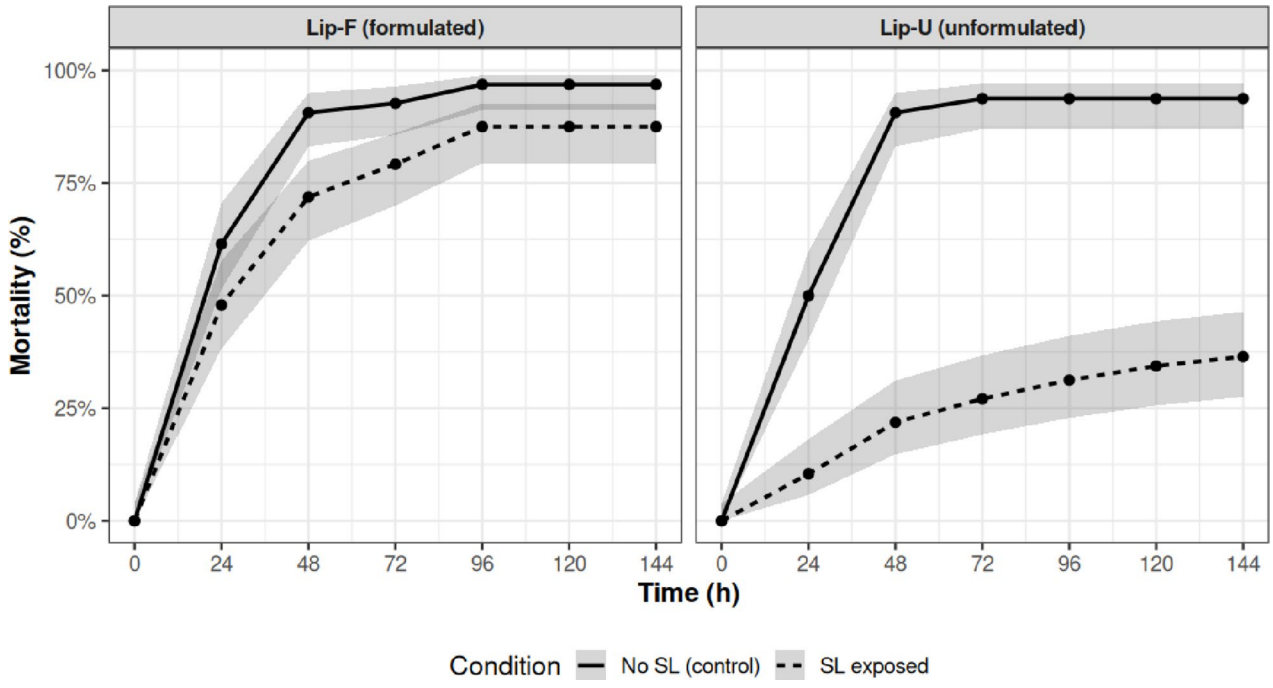


Fig. 8. *S. frugiperda* mortality over time after sunlight treatment. Cumulative mortality (%) of L2 larvae exposed to Lip-F (formulated), and Lip-U (unformulated) bioinsecticide preparations measured from 24 to 144 h. Solid lines represent non-exposed controls (No SL), dashed lines represent SL-exposed samples. Shaded ribbons indicate pooled Wilson 95% confidence intervals computed from cumulative deaths summed across four independent repetitions ($n = 24$ larvae per replicate, and condition).

is typically growth-limiting. Despite this, the Lip strain achieved high final cell density, and complete sporulation. This suggests that the rich carbon content, and micronutrients in the WB medium compensated for any nitrogen shortfall. In sum, our off-gas profiles, and production kinetics match prior reports that the WB-based medium effectively replaces synthetic media for Bt fermentation, driving the characteristic aerobic growth, and nutrient-limited sporulation phases that yield high spore, and Cry-protein[14].

Beyond supporting biological interpretation, the synchronized time series of online physicochemical signals (pO_2 under controlled aeration/agitation, and off-gas–derived r_{CO2}/r_{O2}) together with bioperformances readouts (spores, and toxin-associated proteins) constitute the core dataset required for dynamic, and hybrid model validation. Recent work on dynamic hybrid modelling (DHM) for Bt biopesticide production on industrial substrates, including WB, couples mechanistic mass balances with data-driven estimators of protein/spore kinetics, and emphasizes that accurate DHM construction depends on sufficiently dense experimental trajectories for the key state variables (biomass/substrate/protein/spores), and on reliable phase-transition information from growth, sporulation to lysis[34]. Off-gas monitoring is particularly valuable here because CO_2 in the exhaust gas has been shown to track the transition between vegetative growth, sporulation, and mature spore/crystal release, providing high-frequency "soft-sensor" information that strengthens identifiability, and makes models more transferable to scale-up, and control contexts[35].

After validating that the upstream process reliably reaches the intended trajectory, the next critical step is to verify that downstream processing does not compromise the two main "active" fractions of Bt products-viable spore, and Cry proteins-because both can be sensitive to thermal, and desiccation stress. Spray drying is often associated with losses that depend strongly on process severity, especially outlet temperature, and matrix composition. Studies have shown measurable reductions in Bt spore viability, and crystal-protein content under harsher spray drying conditions, while milder settings, and protective additives can bring performance close to freeze-drying[36]. In this context the agreement across complementary QC readouts—including total and heat-resistant CFU, Bradford protein quantification, SDS–PAGE profiles, Cry-band densitometry, and biological activity—supports the conclusion that the spray-drying workflow preserved biologically relevant product quality rather than merely generating a physically stable powder. More broadly, the findings align with the logic established in recent fluid bed–dried formulation work[14], where a WB-based production combined with a downstream drying/formulation strategy maintained biologically relevant quality, and enabled robust bioactivity benchmarks against Delfin®.

SDS–PAGE analysis revealed a clear, and well-defined protein banding pattern in the formulated sample. A prominent intense band was observed in the high molecular weight region, consistent with the expected size range of Cry proteins, accompanied by additional discrete bands at lower molecular weights. The absence of extensive band smearing or the appearance of multiple low-molecular-weight fragments indicates that no significant protein degradation occurred during fermentation, and downstream processing. The preservation of distinct bands, and their relative intensity confirms the structural integrity of the protein fraction in the final formulation, in agreement with the total protein quantification results.

Estimation of Cry protein content by densitometric analysis of the expected Cry bands (Table 2) yielded lower values than those obtained by total soluble protein quantification, as expected. This difference reflects the fact that Bradford analysis after NaOH treatment measures the overall pool of alkali-solubilized proteins, including Cry proteins together with other soluble protein components released from the spore-crystal preparation, whereas densitometry specifically estimates the intensity of the visible Cry bands on the SDS-PAGE gel. The similar densitometric Cry values obtained for both samples, despite differences in total soluble protein concentration, indicate that total protein content cannot be used as a direct proxy for Cry protein concentration.

Preservation of biological quality alone does not determine the performance of a formulated product, where downstream processing also creates the particle architecture that controls powder handling, reconstitution, and behaviour in aqueous suspension.

The morpho-granulometric data show that the apparent "fineness" of the powders depends strongly on whether particle size is interpreted from number-based or volume-based distributions, and this distinction is important for interpreting how formulation design affects powder architecture, handling, and behaviour after reconstitution. In the dry state, the number-based distributions indicate that Lip-U, and Lip-F are dominated by a ~ 10–20 µm population and are therefore contain a numerically dominant population of smaller particles than the commercial reference. However, the volume-based distributions reveal that a relatively small fraction of large entities carries a disproportionate share of the total mass/volume, meaning that coarse agglomerates (or granule-like structures) remain formulation-relevant even when number-based metrics appear similar. This "hidden" coarse tail is fully consistent with the behaviour reported for the fluid bed–dried Lip formulation described by Nasreddine at al.[14], where all dry powders were multimodal, and broad, and where Delfin® displayed the highest coarse contribution by number while volume fractions were dominated by particles > 30 µm interpreted as granulation/agglomeration during downstream processing, and formulation.

After resuspension (wet way), the key outcome is the markedly improved dispersion of Lip-based products relative to Delfin®. The number-based distributions shift into the 1–2 µm range, and in this size class a substantial portion of the measured "fine fraction" is expected to correspond to biological units (single spores, and spore–crystal complexes) rather than carrier dust. This interpretation is supported by published measurements showing spores/crystals in the micrometre range for Bt, which overlaps the population < 5 µm captured by imaging-based granulometry[37]. Crucially, the volume-based distributions demonstrate that Delfin® retains a persistent coarse fraction in suspension, including particles > 100 µm, whereas Lip-F show no detectable > 100 µm volume fraction, indicating extensive disaggregation during wet dispersion and a lower persistence of structures above 100 µm in the reconstituted suspension, and reduced aggregation persistence in the spray suspension. This reproduces an important physical distinction previously observed for the fluid bed–dried Lip product, elimination of persistent insolubilized coarse particles in the applied suspension state, suggesting that this is a robust property of the Lip-

based formulation strategy rather than an artefact of one specific drying technology[14]. The dry- and wet-way measurements therefore describe different physical states of the products: dry-way analysis characterizes powder architecture and agglomeration, whereas wet-way analysis characterizes the particle population remaining after reconstitution. These descriptors are relevant to handling and dispersion but should not be considered direct predictors of biological efficacy.

From an operator-safety standpoint, the presence of sub-5 µm particles is relevant because occupational aerosol conventions define inhalable, thoracic, and respirable fractions based on aerodynamic diameter (not geometric size), and these fractions are typically evaluated via standardized dustiness methods for bulk materials (EN 15051-2:2013). Importantly, because the fine population in Bt powders can substantially overlap the intrinsic size of spores/crystals, a high number-based fraction < 5 µm does not automatically imply excessive formation of respirable carrier fine rather it highlights the need to interpret number-, and volume-based distributions together, and—if required for regulatory dossiers—to complement geometric granulometry with dustiness/aerodynamic assessments (ISO 7708:1995). The improved dispersion characteristics of the Lip-based formulations should be interpreted alongside their broader biosafety evidence base. Recent toxicological/ecotoxicological assessments of fluid-bed Lip formulations reported low adverse effects in aquatic non-target assays compared with the commercial reference, suggesting that improved physical functionality was not accompanied by evident additional hazard signals in the previously tested assays[38].

The efficacy of Bt–based products depend not only on intrinsic toxicity but also on formulation-driven properties that control suspension stability, spray-tank homogeneity, deposition on foliage, and persistence of active components after application. Static multiple light scattering (SMLS) measurements obtained using the Turbiscan instrument provide a sensitive means of probing these formulation-relevant processes by resolving sedimentation, and clarification kinetics along the sample height under quiescent conditions[23]. Such measurements allow differentiation among uniform clarification, front-like settling, and structurally evolving sediments-modes that have distinct implications for product handling and may influence active-ingredient homogeneity during application.

In this framework, Lip-U represents an unformulated baseline corresponding to a raw spray-dried biomass. Its pronounced bottom-zone backscattering signature, and large cumulative ΔBS response are consistent with the formation of an optically dense, and continuously evolving sediment structure. Similar behaviour has been reported for concentrated biological, and colloidal suspensions in which fine particles, and cohesive aggregates promote gradual consolidation rather than rapid clarification of the bulk[39,40]. From an application perspective, such behaviour may lead to extended turbidity in the spray liquid but also to the development of a structured sediment that requires substantial agitation to redisperse, potentially generating concentration gradients and variable dose delivery if adequate agitation is not maintained[41].

The comparison between the formulated prototype Lip-F and Delfin® revealed distinct suspension-destabilization mechanisms resulting from their different formulations and particle architectures. Delfin® exhibits early, and spatially uniform clarification, a behaviour indicative of rapid decantation, and efficient packing of sedimented particles. Uniform clarification profiles of this type have been associated with relatively coherent settling, and fast stabilization of the sediment bed. While such behaviour yields a visually clear supernatant, previous formulation studies have emphasized that rapid clarification can increase the risk of concentration gradients in spray tanks under insufficient agitation, potentially leading to variable delivery of the active ingredient during application[42]. By contrast, Lip-F displays delayed, and more localized clarification together with reduced bottom-zone densification compared to Lip-U. The inclusion of lactose is likely to play a key role in this behaviour, as carbohydrate matrices are widely used in microbial formulations to stabilize biological material during drying, and rehydration, and to modulate interparticle interactions upon dispersion[43]. Such excipients can reduce excessive aggregation, and alter sediment packing, leading to progressive clarification, and less compact sediment formation, features that have been linked to improved re-dispersibility, and handling properties in plant protection formulations.

The presence of TiO_2 in Lip-F further strengthens an efficacy-oriented interpretation of the observed stability patterns. TiO_2 has been extensively reported as an effective ultraviolet protective additive for *Bt* formulations, enhancing spore survival, and toxin persistence under ultraviolet exposure[44]. The Turbiscan data indicate that, despite the high refractive index of TiO_2[45], Lip-F does not exhibit exaggerated bottom-zone backscattering compared with the baseline formulation, suggesting that TiO_2 is integrated into a formulation matrix that modifies sediment structure rather than simply increasing optical contrast. This balance between modified sedimentation behaviour, and sunlight protection is particularly relevant for field efficacy, where persistence on leaf surfaces, and resistance to environmental degradation are critical determinants of biological performance[46].

Taken together, the SMLS profiles support the hypothesis that Lip-F produces a different balance between front propagation, bulk clarification, and bottom-zone accumulation than either Lip-U or Delfin®. This pattern may be relevant to spray-liquid homogeneity and redispersibility, although these application properties and the concentrations of viable spores or Cry proteins remaining in suspension were not measured directly.Slower, front-like clarification combined with moderated bottom-zone densification may contribute to more uniform delivery during spray preparation, and application, while TiO_2 contributes to enhanced post-application persistence through sunlight protection. Similar relationships between formulation-driven stability, handling properties, and biological efficacy have been reported for microbial biopesticides, where improved dispersion behaviour translated into more consistent insect control[47].

Overall, while Turbiscan measurements do not directly quantify biological activity, they provide formulation-relevant indicators that align with established links between physical stability, application behaviour, and efficacy. Within this context, Lip-U serves as a useful baseline for intrinsic biomass behaviour, Delfin® exemplifies rapid, and uniform sedimentation, and Lip-F emerges as a formulation that strategically modulates sedimentation dynamics while incorporating proven efficacy-enhancing components. The biological performance of Lip-F

cannot be attributed to particle size or suspension behaviour alone. Instead, it may reflect the combined contribution of the formulation matrix, preservation of the active biological material, particle architecture after reconstitution, and suspension behaviour. The particle-size and SMLS measurements should therefore be interpreted as complementary physicochemical descriptors rather than as a direct ranking of expected biological efficacy. The functional relevance of the upstream and formulation processes was subsequently evaluated through comparative bioassays against five lepidopteran target species. Across the five target pests, the baseline Probit bioassays support a clear efficacy message, that Lip-F retains commercial-benchmark activity across taxonomically diverse Lepidoptera, and where differences occur, they are expressed primarily as potency shifts rather than altered dose–response shape. This interpretation is strengthened by the parallelism outcomes—non-significant slope differences imply that the formulations behave similarly in how mortality scales with dose, which is consistent with a shared Cry-toxin mode of action, and a comparable "delivery/toxicity" relationship across products. In the Bt literature, such patterns are common: commercial Btk products can differ by several-fold in LC_{50} against the same insect, and these differences are often attributed to formulation composition, and Cry-profile rather than a fundamentally different response mechanism[48]. The absence of treatment separation in species such as *S. frugiperda* is also biologically plausible given the known variability in susceptibility of this pest to different Cry proteins, and Cry mixes, where potency depends strongly on toxin type, receptor interactions, and protein stability in the midgut[49]. Where Lip-F diverges from Delfin®, the *O. nubilalis* outcome is particularly meaningful because this species is a classical Btk/Cry1Ab-responsive target, and modest formulation-driven potency improvements have been reported when Cry toxins are protected or better delivered[50]. Together, these baseline efficacy data provide the functional validation needed before interpreting sunlight stability, Lip-F is not only physically stable, and biochemically intact, but also biologically equivalent to Delfin® under non-stressed conditions, thus post-exposure divergence can be attributed credibly to differences in environmental protection rather than initial potency.

Sunlight exposure is a primary reason why Bt products often underperform outside the lab. Sunlight (especially UV-A/UV-B) accelerates loss of spore viability, and Cry protein integrity, shortening residual activity on foliage. This limitation has been recognized for decades, including early wavelength-dependent inactivation studies, and the long-standing emphasis on "sunscreening" systems for Bt[51]. The exposure dataset shows that the formulated product (Lip-F) is substantially more resilient than the unformulated biomass (Lip-U) at multiple, convergent levels (CFU, protein integrity, and functional killing), which is exactly the expected signature of effective sunlight protective formulation. At the CFU level, Lip-F exhibits a much smaller sunlight-induced log reduction than Lip-U, indicating that the formulation protects spore-associated viability rather than simply preserving a stable powder. This is consistent with the formulation literature where sunlight protective architectures (encapsulation, UV absorbers/scatterers) measurably increase post-SL survival of Bt spores compared to unprotected controls[44]. In particular, TiO_2 has direct precedent as a sunlight protectant for Bt, a Scientific Reports study comparing different TiO_2 polymorphs showed significantly higher larval mortality after prolonged UV-A exposure when Bt was combined with TiO_2 (with performance depending on the TiO_2 form), supporting TiO_2's role as a practical photoprotective additive[52]. The protection signal is also visible at the protein/SDS–PAGE level. Total protein retention after exposure is higher in Lip-F than Lip-U, and the post-exposure SDS–PAGE outcome (marked degradation in Lip-U vs. preserved pattern in Lip-F) indicates that formulation mitigates sunlight-driven damage to the toxin-associated protein fraction. Most compellingly, the formulation advantage persists at the bioassay level, where sunlight exposure causes a dramatic, sustained loss of killing for Lip-U but only a moderate effect for Lip-F (endpoint, and time-to-effect). This pattern is exactly what photoprotection is supposed to achieve, not merely keeping CFU high, but maintaining functional potency over time after realistic light stress.

Overall, the integrated upstream–downstream dataset demonstrates a robust, integrated Bt production and formulation workflow with clear potential for future scale-up evaluation in which process monitoring, product quality, physical functionality, and biological performance are coherently aligned. Online pO_2 and off-gas (rO_2V/rCO_2V) trajectories reliably captured the transition from oxidative growth to sporulation, providing a practical basis to optimize bioproduction by using gas analysis (with pH regulation) to detect the fall-over into sporulation, and then reducing operational intensity once sporulation begins—i.e., stopping pH regulation, lowering mixing to a minimal value, and stopping aeration or maintaining only a minimal VVM—to stimulate sporulation while minimizing unnecessary energy input during late, low-activity phases. Downstream, quality control confirmed preservation of the active fractions (spores, and Cry proteins), while morphogranulometry, and suspension suspendability analyses indicated that formulation design governs dispersion, and sedimentation behaviour relevant to spray application. However, these physicochemical characteristics were not independently manipulated or quantitatively correlated with insecticidal efficacy in the present study. Their contribution to biological performance should therefore be considered formulation-relevant but not causally demonstrated, and no single particle-size or suspension parameter can be identified as the driver of efficacy. Functionally, the bioassays confirm that the improved physicochemical properties of the Lip-based formulation are achieved without compromising insecticidal performance relative to the benchmark product. For *S. exigua*, Lip-U, Lip-F, and Delfin® showed statistically comparable LC_{50} values, supporting comparable baseline efficacy under standardized laboratory conditions. For *O. nubilalis*, Lip-U, and Delfin® remained equivalent, while Lip-F showed higher activity, indicating that formulation can enhance potency in specific host contexts without altering the overall dose–response shape. For *G. molesta*, Lip-U tended to be less toxic than Lip-F, whereas both products remained comparable to Delfin® within the confidence intervals. Taken together, these results support the main conclusion of the study that Lip-F matches the commercial reference in baseline efficacy, while offering more favourable formulation-driven characteristics—a finer and more homogeneous dispersed particle population, modified suspension behaviour, and substantially improved resistance to sunlight exposure. Although the individual contribution of these physicochemical attributes to efficacy cannot be resolved from the present

experimental design, their combined occurrence supports further evaluation of Lip-F for consistent delivery and persistence under field-relevant conditions.

Data availability

The datasets used and/or analysed during the current study available from the corresponding author on reasonable request.

Received: 13 May 2026; Accepted: 26 October 2026
Published online: 09 November 2026

References

1. Ayilara, M. S. et al. Biopesticides as a promising alternative to synthetic pesticides: A case for microbial pesticides, phytopesticides, and nanobiopesticides. *Front. Microbiol.***14**, 1040901. https://doi.org/10.3389/fmicb.2023.1040901 (2023).
2. Vachon, V., Laprade, R. & Schwartz, J. L. Current models of the mode of action of *Bacillus thuringiensis* insecticidal crystal proteins: A critical review. *J. Invertebr. Pathol.***111**, 1–12. https://doi.org/10.1016/j.jip.2012.05.001 (2012).
3. Polanczyk, R. A., Silva, R. F. P. & Fiuza, L. M. Effectiveness of *Bacillus thuringiensis* strains against *Spodoptera frugiperda* (Lepidoptera: Noctuidae). *Brazilian J. Microbiol.***31**, 165–167. https://doi.org/10.1590/S1517-83822000000300003 (2000).
4. González-Cabrera, J., Mollá, O., Montón, H. & Urbaneja, A. Efficacy of Bacillus thuringiensis (Berliner) in controlling the tomato borer, Tuta absoluta (Meyrick) (Lepidoptera: Gelechiidae). *BioControl***56**, 71–80. https://doi.org/10.1007/s10526-010-9310-1 (2011).
5. Ricietto, A. P. S., Gomis-Cebolla, J., Vilas-Bôas, G. T. & Ferré, J. Susceptibility of *Grapholita molesta* (Busck, 1916) to formulations of *Bacillus thuringiensis*, individual toxins and their mixtures. *J. Invertebr. Pathol.***141**, 1–5. https://doi.org/10.1016/j.jip.2016.09.006 (2016).
6. Avignone-Rossa, C., Arcas, J. & Mignone, C. *Bacillus thuringiensis* growth, sporulation and δ-endotoxin production in oxygen-limited and non-limited cultures. *Biotechnol. Lett.***14**, 301–304. https://doi.org/10.1007/BF01201884 (1992).
7. Oliveira, J. L. et al. Performance insights into spray-dryer microencapsulated *Bacillus thuringiensis* Cry pesticidal proteins with gum arabic and maltodextrin for effective pest control. *Appl. Microbiol. Biotechnol.***108**, 181. https://doi.org/10.1007/s00253-023-12990-7 (2024).
8. Oliveira, J. L., Fraceto, L. F., Bravo, A. & Polanczyk, R. A. Encapsulation strategies for *Bacillus thuringiensis*: From now to the future. *J. Agric. Food Chem.***69**, 4564–4577. https://doi.org/10.1021/acs.jafc.0c07118 (2021).
9. Vicente, J., Pinto, J., Menezes, J. & Gaspar, F. Fundamental analysis of particle formation in spray drying. *Powder Technol.***247**, 1–7. https://doi.org/10.1016/j.powtec.2013.06.038 (2013).
10. Wang, A. et al. Modification of sedimentation and bioaccumulation behavior as an efficient strategy to modulate the toxicity of pyraclostrobin to zebrafish (Danio rerio). *Environ. Pollut.***322**, 121164. https://doi.org/10.1016/j.envpol.2023.121164 (2023).
11. Luo, J. et al. Analysis of particle size regulating the insecticidal efficacy of phoxim polyurethane microcapsules on leaves. *ACS Sustainable Chem. & Engineering.* **6**, 17194–17203. https://doi.org/10.1021/acssuschemeng.8b04567 (2018).
12. Ragasruthi, M. et al. *Bacillus thuringiensis* (Bt)-based biopesticide: Navigating success, challenges, and future horizons in sustainable pest control. *Sci. Total Environ.***954**, 176594. https://doi.org/10.1016/j.scitotenv.2024.176594 (2024).
13. Vineela, V., Nataraj, T., Reddy, G. & Vimala Devi, P. S. Enhanced bioefficacy of *Bacillus thuringiensis* var. kurstaki against *Spodoptera litura* (Lepidoptera: Noctuidae) through particle size reduction and formulation as a suspension concentrate. *Biocontrol Sci. Technol.***27**, 58–69. https://doi.org/10.1080/09583157.2016.1247433 (2017).
14. Nasreddine, R. et al. Bioactivity and physical investigation of a novel fluid bed-dried *Bacillus thuringiensis kurstaki* formulation. *J. Invertebr. Pathol.* 108547. https://doi.org/10.1016/j.jip.2026.108547 (2026).
15. El Khoury, M. et al. Isolation and characterization of a new *Bacillus thuringiensis* strain Lip harboring a new cry1Aa gene highly toxic to *Ephestia kuehniella* (Lepidoptera: Pyralidae) larvae. *Arch. Microbiol.***196**, 435–444. https://doi.org/10.1007/s00203-014-0981-3 (2014).
16. Fayad, N. et al. Complete genome sequences of two *Bacillus thuringiensis* serovar *kurstaki* strains isolated from Lebanon and Tunisia, highly toxic against lepidopteran larvae. *Microbiol. Resource Announcements*. **12**, e00060–e00023. https://doi.org/10.1128/MRA.00060-23 (2023).
17. Sanders, E. R. Aseptic laboratory techniques: Plating methods. *J. Visualized Experiments*. e3064. https://doi.org/10.3791/3064 (2012).
18. Bradford, M. M. A rapid and sensitive method for the quantitation of microgram quantities of protein utilizing the principle of protein-dye binding. *Anal. Biochem.***72**, 248–254. https://doi.org/10.1016/0003-2697(76)90527-3 (1976).
19. Eski, A., Demirbağ, Z. & Demir, İ. Microencapsulation of an indigenous isolate of *Bacillus thuringiensis* by spray drying. *J. Microencapsul.***36**, 1–9. https://doi.org/10.1080/02652048.2019.1572238 (2019).
20. Warda, A. K., Tempelaars, M. H. & Abee, T. Nierop Groot, M. N. Recovery of heat-treated *Bacillus cereus* spores is affected by matrix composition and factors with putative functions in damage repair. *Front. Microbiol.***7**, 1096. https://doi.org/10.3389/fmicb.2016.01096 (2016).
21. Barssoum, R. et al. Biochemical limitations of *Bacillus thuringiensis*-based biopesticides production in a wheat bran culture medium. *Res. Microbiol.***174**, 104043. https://doi.org/10.1016/j.resmic.2023.104043 (2023).
22. Timoumi, A. et al. Comparison of methods to explore the morphology and granulometry of biological particles with complex shapes: Interpretation and limitations. *Powder Technol.***415**, 118067. https://doi.org/10.1016/j.powtec.2022.118067 (2023).
23. Liu, J. et al. Turbiscan Lab® Expert analysis of the biological demulsification of a water-in-oil emulsion by two biodemulsifiers. *J. Hazard. Mater.***190**, 214–221. https://doi.org/10.1016/j.jhazmat.2011.03.028 (2011).
24. Mekoue Nguela, J., Pereira, Y. F., Sieczkowski, N. & Vernhet, A. Application of Turbiscan Lab® to study the mechanism of fining in red wine using a specific yeast protein extract: A comparison with gelatine. *Colloids Surf., A.* **699**, 134649. https://doi.org/10.1016/j.colsurfa.2024.134649 (2024).
25. Hernández-Martínez, P., Ferré, J. & Escriche, B. Susceptibility of *Spodoptera exigua* to nine toxins from *Bacillus thuringiensis*. *J. Invertebr. Pathol.***97**, 245–250. https://doi.org/10.1016/j.jip.2007.11.001 (2008).
26. Finney, D. J. *Probit Analysis* 3rd edn (Cambridge University Press, 1971).
27. Mantel, N. & Haenszel, W. Statistical aspects of the analysis of data from retrospective studies of disease. *J. Natl Cancer Inst.***22**, 719–748 (1959). https://pubmed.ncbi.nlm.nih.gov/13655060/
28. Wickham, H. *ggplot2: Elegant Graphics for Data Analysis* (Springer, 2009). https://link.springer.com/book/10.1007/978-3-319-24277-4
29. Wickham, H., François, R., Henry, L., Müller, K. & Vaughan, D. dplyr: A Grammar of Data ManipulationR package (2023). https://dplyr.tidyverse.org/
30. Preisler, H. K. & Robertson, J. L. Analysis of time-dose-mortality data. *J. Econ. Entomol.***82**, 1534–1542. https://doi.org/10.1093/jee/82.6.1534 (1989).

31. Boniolo, F. S. et al. Oxygen supply in *Bacillus thuringiensis* fermentations: Bringing new insights on their impact on sporulation and δ-endotoxin production. *Appl. Microbiol. Biotechnol.***94**, 625–636. https://doi.org/10.1007/s00253-011-3746-9 (2012).
32. Razo Flores, E. R., Pérez, F. & de la Torre, M. Scale-up of *Bacillus thuringiensis* fermentation based on oxygen transfer. *J. Ferment. Bioeng.***83**, 561–564. https://doi.org/10.1016/S0922-338X(97)81137-3 (1997).
33. Fayad, N., Abboud, J., Driss, F., Louka, N. & Kallassy Awad, M. Optimization of culture conditions and wheat bran class selection in the production of *Bacillus thuringiensis*-based biopesticides. *Fermentation***8**, 666. https://doi.org/10.3390/fermentation8120666 (2022).
34. Figueroa-Cardona, S., Robles-Rodriguez, C. E., Fillaudeau, L., El-Jeni, R. & Aceves-Lara, C. A. Dynamic hybrid model for biopesticides production using industrial substrate. *Chem. Eng. Trans.***119**https://doi.org/10.3303/CET25119058 (2025).
35. Mounsef, J. R., Salameh, D., Louka, N., Brandam, C. & Lteif, R. The effect of aeration conditions, characterized by the volumetric mass transfer coefficient kLa, on the fermentation kinetics of *Bacillus thuringiensis kurstaki*. *J. Biotechnol.***210**, 100–106. https://doi.org/10.1016/j.jbiotec.2015.06.387 (2015).
36. Zhou, X., Dong, J., Gao, J. & Yu, Z. Activity-loss characteristics of spores of *Bacillus thuringiensis* during spray drying. *Food Bioprod. Process.***86**, 37–42. https://doi.org/10.1016/j.fbp.2007.10.017 (2008).
37. Loutfi, H. et al. Morphological study of *Bacillus thuringiensis* crystals and spores. *Appl. Sci.***11**, 155. https://doi.org/10.3390/app11010155 (2021).
38. Dhaouadi, S. et al. Effects of new Btk-based formulations BLB1 and Lip on aquatic non-target organisms. *Biology***13**https://doi.org/10.3390/biology13100824 (2024).
39. Vie, R., Azema, N., Quantin, J. C., Touraud, E. & Fouletier, M. Study of suspension settling: An approach to determine suspension classification and particle interactions. *Colloids Surf., A*. **298**, 192–200. https://doi.org/10.1016/j.colsurfa.2006.10.074 (2007).
40. Lemahieu, G., Sentis, M. P., Brambilla, G. & Meunier, G. Coupling static multiple light scattering (SMLS) analysis with the Hansen approach for the rationalization of the dispersibility and colloidal stability of TiO2 particle dispersions. *Colloids Surf., A*. **688**, 133630. https://doi.org/10.1016/j.colsurfa.2024.133630 (2024).
41. Hynes, R. K. & Boyetchko, S. M. Research initiatives in the art and science of biopesticide formulations. *Soil. Biology Biochemistry*. **38**, 845–849. https://doi.org/10.1016/j.soilbio.2005.07.003 (2006).
42. Knowles, A. Recent developments of safer formulations of agrochemicals. *Environmentalist***28**, 35–44. https://doi.org/10.1007/s10669-007-9045-4 (2008).
43. Mascarin, G. M. et al. Advances in submerged liquid fermentation and formulation of entomopathogenic fungi. *Appl. Microbiol. Biotechnol.***108**, 451. https://doi.org/10.1007/s00253-024-13287-z (2024).
44. Jalali, E., Maghsoudi, S. & Noroozian, E. Ultraviolet protection of *Bacillus thuringiensis* through microencapsulation with Pickering emulsion method. *Sci. Rep.***10**, 20633. https://doi.org/10.1038/s41598-020-77721-8 (2020).
45. Diebold, U. The surface science of titanium dioxide. *Surf. Sci. Rep.***48**, 53–229. https://doi.org/10.1016/S0167-5729(02)00100-0 (2003).
46. Maghsoudi, S. & Jalali, E. Noble UV protective agent for *Bacillus thuringiensis* based on a combination of graphene oxide and olive oil. *Sci. Rep.***7**, 11019. https://doi.org/10.1038/s41598-017-11080-9 (2017).
47. Lacey, L. A. et al. Insect pathogens as biological control agents: Back to the future. *J. Invertebr. Pathol.***132**, 1–41. https://doi.org/10.1016/j.jip.2015.07.009 (2015).
48. Mohan, M. & Gopalan, G. G. Toxicity of *Bacillus thuringiensis* strains and commercial formulations to the diamondback moth, *Plutella xylostella* (L). *Crop Prot.***20**, 311–316. https://doi.org/10.1016/S0261-2194(00)00157-5 (2001).
49. Gómez, I. et al. Enhancement of Bacillus thuringiensis Cry1Ab and Cry1Fa toxicity to *Spodoptera frugiperda* by domain III mutations indicates two limiting steps in toxicity as defined by receptor binding and protein stability. *Appl. Environ. Microbiol.***84**https://doi.org/10.1128/AEM.01393-18 (2018).
50. Jalali, E., Bel, Y., Maghsoudi, S., Noroozian, E. & Escriche, B. Enhancing insecticidal efficacy of *Bacillus thuringiensis* Cry1Ab through pH-sensitive encapsulation. *Appl. Microbiol. Biotechnol.***107**, 6407–6419. https://doi.org/10.1007/s00253-023-12723-w (2023).
51. Griego, V. M. & Spence, K. D. Inactivation of *Bacillus thuringiensis* spores by ultraviolet and visible light. *Appl. Environ. Microbiol.***35**, 906–910. https://doi.org/10.1128/aem.35.5.906-910.1978 (1978).
52. Jalali, E., Maghsoudi, S. & Noroozian, E. A novel method for biosynthesis of different polymorphs of TiO2 nanoparticles as a protector for *Bacillus thuringiensis* from ultraviolet. *Sci. Rep.***10**, 426. https://doi.org/10.1038/s41598-019-57407-6 (2020).

Acknowledgements

The authors gratefully acknowledge Rosa Meinhold-Ernst, Chiara Weber, Astrid von Galen, Juliana Penther from Julius Kühn Institute, Institute for Biological Control, and Rosa Maria Gonzales from the CBP group, University of Valencia for their huge technical support.

Author contributions

Rayan Nasreddine: Writing – original draft, Visualization, Validation, Methodology, Investigation, Formal analysis, Conceptualization. Gül Ayyildiz: Methodology, Investigation, Data curation. Zhanerke Amangeldi: Methodology, Investigation. Cecilia Peralta: Methodology, Investigation. Asime Filiz Caliskan Keçe: Methodology, review & editing. Mireille Kallassy Awad: Writing – review & editing, Visualization, Supervision, Methodology, Investigation. Luc Fillaudeau: Writing – review & editing, Visualization, Supervision, Methodology, Investigation. Baltasar Escriche: Writing – review & editing, Visualization, Supervision, Methodology, Investigation. Dietrich Stephan: Writing – review & editing, Validation, Supervision, Resources, Project administration, Methodology, Funding acquisition, Data curation, Conceptualization.

Funding

Open Access funding enabled and organized by Projekt DEAL. This research received funding from the project "SAFWA-Alternative Biopesticides for Safe Integrated Pest and Water Management around the Mediterranean", which is funded by the PRIMA program. The PRIMA program is supported by the European Union. CBP operations were financed by the Spanish National Funding Agency (AEI) (MICIU/AEI/https://doi.org/10.13039/501100011033 with the grant PCI2023-143439), and by the German Federal Ministry of Research, Technology, and Space (BMFTR) under the funding code 02WPM1684 (SAFWA).

Declarations

Competing interests
The authors declare no competing interests.

Disclosure statement
The authors declare no conflict of interest. This work was supported by SAFWA-Prima project. The funders had no role in the design of the study, collection, analysis, or interpretation of data, or in the decision to publish the results.

Additional information
Supplementary Information The online version contains supplementary material available at https://doi.org/10.1038/s41598-026-78427-z.

Correspondence and requests for materials should be addressed to D.S.

Reprints and permissions information is available at www.nature.com/reprints.

Publisher's Note Springer Nature remains neutral with regard to jurisdictional claims in published maps and institutional affiliations.

Open Access This article is licensed under a Creative Commons Attribution 4.0 International License, which permits use, sharing, adaptation, distribution and reproduction in any medium or format, as long as you give appropriate credit to the original author(s) and the source, provide a link to the Creative Commons licence, and indicate if changes were made. The images or other third party material in this article are included in the article's Creative Commons licence, unless indicated otherwise in a credit line to the material. If material is not included in the article's Creative Commons licence and your intended use is not permitted by statutory regulation or exceeds the permitted use, you will need to obtain permission directly from the copyright holder. To view a copy of this licence, visit http://creativecommons.org/licenses/by/4.0/.

© The Author(s) 2026